Microbiome

RESEARCH

Open Access

Bacillus species are core microbiota of resistant maize cultivars that induce host metabolic defense against corn stalk rot

Xinyao Xia[1,2,3†], Qiuhe Wei[1†], Hanxiang Wu[1†], Xinyu Chen[1], Chunxia Xiao[1], Yiping Ye[1], Chaotian Liu[1], Haiyue Yu[1], Yuanwen Guo[1], Wenxian Sun[2] and Wende Liu[1*]

Abstract

Background Microbes colonizing each compartment of terrestrial plants are indispensable for maintaining crop health. Although corn stalk rot (CSR) is a severe disease affecting maize (*Zea mays*) worldwide, the mechanisms underlying host–microbe interactions across vertical compartments in maize plants, which exhibit heterogeneous CSR-resistance, remain largely uncharacterized.

Results Here, we investigated the microbial communities associated with CSR-resistant and CSR-susceptible maize cultivars using multi-omics analysis coupled with experimental verification. Maize cultivars resistant to CSR reshaped the microbiota and recruited *Bacillus* species with three phenotypes against *Fusarium graminearum* including niche pre-emption, potential secretion of antimicrobial compounds, and no inhibition to alleviate pathogen stress. By inducing the expression of *Tyrosine decarboxylase 1* (*TYDC1*), encoding an enzyme that catalyzes the production of tyramine and dopamine, *Bacillus* isolates that do not directly suppress pathogen infection induced the synthesis of berberine, an isoquinoline alkaloid that inhibits pathogen growth. These beneficial bacteria were recruited from the rhizosphere and transferred to the stems but not grains of the CSR-resistant plants.

Conclusions The current study offers insight into how maize plants respond to and interact with their microbiome and lays the foundation for preventing and treating soil-borne pathogens.

Keywords *Bacillus*, Corn stalk rot, Compartments, Microbiome, Resistance

† Xinyao Xia, Qiuhe Wei and Hanxiang Wu contributed equally to this work.

*Correspondence:
Wende Liu
liuwende@caas.cn
[1] State Key Laboratory for Biology of Plant Diseases and Insect Pests, Key Laboratory of Integrated Pest Management in Crops, Ministry of Agriculture and Rural Affairs, Institute of Plant Protection, Chinese Academy of Agricultural Sciences, Beijing 100193, China
[2] Department of Plant Pathology, Ministry of Agriculture Key Laboratory of Pest Monitoring and Green Management and Joint International Research Laboratory of Crop Molecular Breeding, Ministry of Education, China Agricultural University, Beijing 100193, China
[3] Key Laboratory for Safety Assessment (Environment) of Agricultural Genetically Modified Organisms, Ministry of Agriculture and Rural Affairs, Institute of Plant Protection, Shandong Academy of Agricultural Sciences, Jinan 250100, China

Background

Corn stalk rot (CSR), an economically destructive soil-borne disease affecting maize (*Zea mays*)-growing areas worldwide, is caused by pathogens such as the fungi *Fusarium* and the oomycete *Pythium*, as well as bacterial species like *Dickeya zeae* and *Pseudomonas aeruginosa* [1–3]. Single or multiple pathogens infect the root vascular bundle via natural openings or wounds, thereby affecting water and nutrient transport and ultimately causing the plant to wilt and die [4]. Due to the wide variety of geographically specific pathogens and local differences in infection routes throughout the growth period, conventional field management measures such as seed coating with chemical fungicides have had limited

success in disease control [5]. Although introducing resistance genes into a host plant through genetic engineering reduces the incidence of disease [6], accordingly, one of the current challenges is to identify appropriate parental resources and stabilize resistance genes in complex and volatile environments [7]. Therefore, there is a need to identify efficient and more natural disease-suppressive methods from the perspective of agroecosystem management.

Microbes are vital to ecosystem health and have effectively colonized plants during the last 400 million years of coevolution with their plant hosts [8, 9]. Plants enhance their resistance to pathogens by reshaping the composition of their associated microbe communities, resulting in the assembly of a stress-alleviating microbiota [10–12]. The plant-mediated "cry for help" hypothesis further highlights the potential for microbes as a significant component of resistance mechanisms, defining an important role for the microbiota in stimulating host resistance to plant diseases and insect pests and tolerance to abiotic stress while promoting growth [13–15]. Specifically, *Trichoderma* fungi colonize the soil and maize roots, thereby reducing the overall number of pathogenic *Fusarium* species [16, 17]. Chili pepper (*Capsicum annuum*) plants infected with *Fusarium* wilt disease recruit beneficial bacteria and mitigate changes in the microbiome in reproductive organs to facilitate the survival of the host and its progeny [18]. These observations suggest that both bacteria and fungi have tremendous potential as biological control agents of CSR [19].

To develop effective disease management strategies, it is imperative to explore the contributions of bacterial and fungal taxa known to improve resistance in plants grown under natural conditions and to identify additional microbes from the "microbial dark matter" [20]. Notably, the genotype-specific characteristics of the endophytic microbiomes in the seed and "resistance legacy" (also known as "soil-borne memory") of the effects of plant–microbe interactions in previous plant generations have been demonstrated [21, 22]. These cross-generational microbes are located in compartments at the two terminals of host (soil and seeds), pointing to multi-mechanistic microbiome heritability [23]. A comprehensive analysis of microbial communities in distinct compartments of maize infected with CSR can provide important information about the sources and heritability of seed endophytic microbes and suggest strategies for CSR prevention.

Initially, a range of resistance levels to CSR were observed among a maize-associated mapping panel (AMP) of 527 cultivars [24] with temperate, tropical, and subtropical genetic backgrounds representing global maize diversity. These 527 cultivars contain different populations, including 33 cultivars for stiff-stock (SS), 143 for non-stiff-stock (NSS), 232 for tropical and semi-tropical (TST), and the left 119 cultivars for mixed, encompassing adequate genetic diversity and covering most variations for the traits of interest (Supplementary Table 1). We hypothesized that the structural and functional adaptation of the microbial communities would differ in CSR-resistant and CSR-susceptible maize cultivars. In the current study, using CSR-resistant and CSR-susceptible maize cultivars, we performed a multi-omics analysis including 16S/ITS amplicon sequencing, metagenomic, and genomic sequencing of host-associated bacterial and fungal communities in the soil (bulk soil and rhizosphere) and plant endogenous tissues (root, stem and grain). We identified core CSR-resistance related microbiota in maize which could alleviate pathogen stress through inducing the synthesis of isoquinoline alkaloid, laying the foundation for the development of biological control methods against this devastating disease.

Results

Specific compartments and CSR-resistance drive the assembly of associated bacterial communities

Our aim is to identify the core taxa of CSR-resistant plants; 40 maize cultivars (with representative phenotypes for CSR) were preliminarily selected from the 527 cultivars for two consecutive years and were inoculated with *Fusarium graminearum* in the root zones (avoiding injuring the roots). We identified pronounced and consistent differences in CSR disease indexes (Supplementary Table 2). Infected maize plants exhibit hollow stems and roots covered with red mycelium, which eventually cause the plant to break (Fig. 1a). Four CSR-resistant (GZL54, GZL185, GZL339, and GZL455, disease incidence = 0%) and four CSR-susceptible (GZL165, GZL200, GZL331, and GZL533, disease incidence > 30%) cultivars were selected for further study. Firstly, pot experiments were employed to validate the importance of soil microbiome to the CSR-resistant cultivars (Extended Data Fig. 1a). With the addition of spore suspensions (10^5 spores/mL) once a week for 3 weeks, the pathogenetic seedlings withered and died; the disease index was recorded by diseased plants accounted for the proportion of total seedling number. All the four CSR-resistant cultivars (GZL54, GZL185, GZL339, and GZL455) showed significantly lower disease indexes in natural soil at seedling stage than those grown in the same soil after sterilization (Wilcoxon rank sum test, $P < 0.05$), suggesting the participation of soil microbiome for CSR-resistant cultivars.

To analyze the bacterial and fungal communities of maize plants that are resistant or susceptible to CSR, we

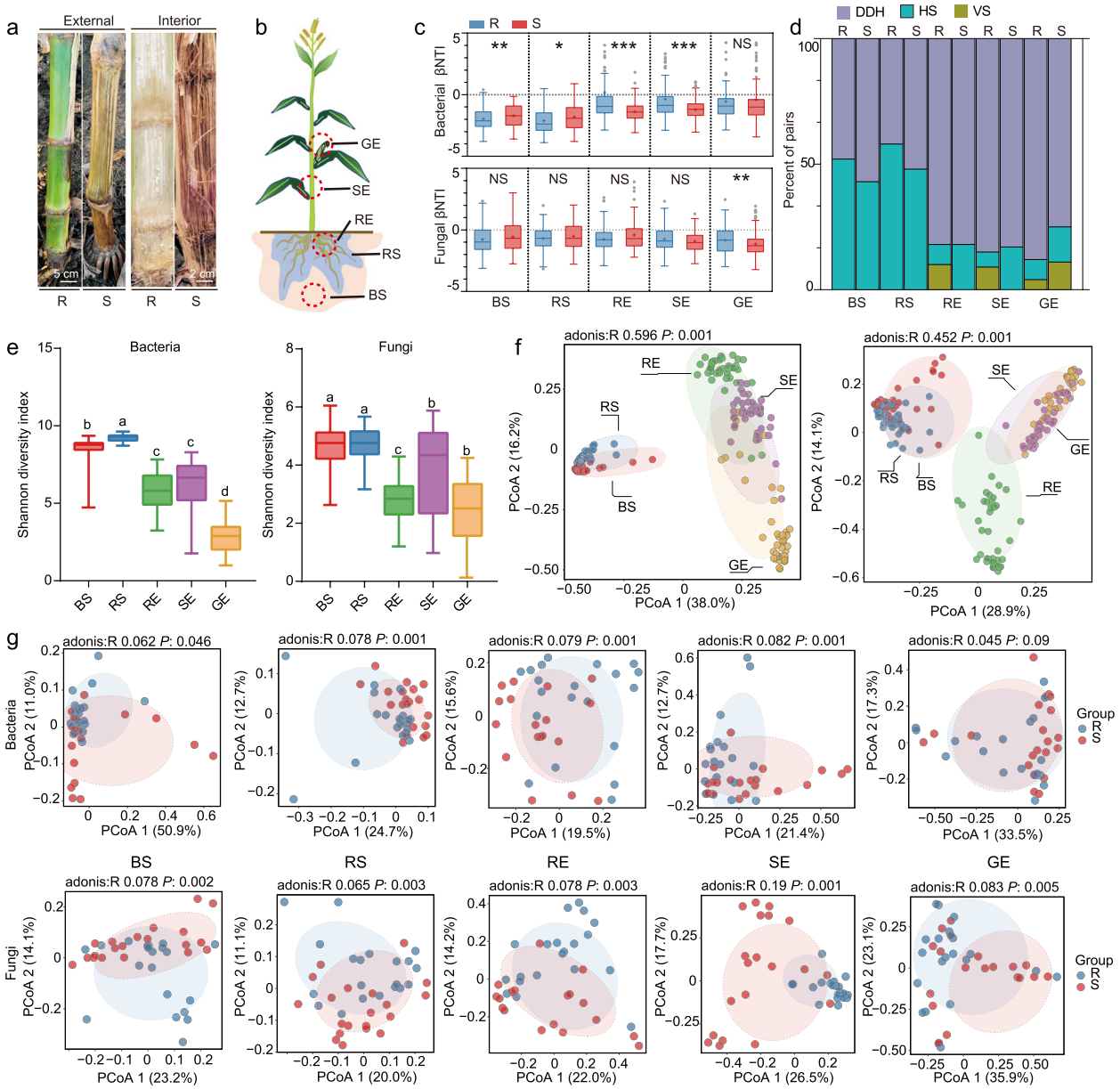

Fig. 1 Effects of CSR-resistance difference on microbiome assembly and diversity in five compartments of maize. **a** Phenotypes of the external surfaces and interiors of maize stems in CSR-resistant (GZL455) and CSR-susceptible (GZL200) individuals. **b** Diagram showing the sampling compartments: BS, bulk soil; RS, rhizosphere soil; RE, root endosphere; SE, stem endosphere; GE, grain endosphere. **c** βNTI calculations of phylogenetic turnover in CSR-resistant and CSR-susceptible samples in the five compartments. *, $P < 0.05$; **, $P < 0.01$; ***, $P < 0.001$ in the Wilcoxon rank sum test ($n = 40$). **d** Relative influence of three community assembly processes among CSR-resistant and CSR-susceptible microbial communities across the five compartments. DDH, drift, dispersal limited, and homogeneous selection (|βNTI| < 2, stochastic processes); HS, homogenizing dispersal (βNTI < −2, deterministic processes); VS, variable selection (βNTI > 2, deterministic processes). **e** Shannon diversity index (SDI) of bacterial and fungal communities in the five compartments. Different letters indicate significant differences (ordinary one-way ANOVA test, $P < 0.05$). **f** Principal coordinates analysis (PCoA) of bacterial (left) and fungal (right) communities based on Bray–Curtis distances. Significant differences among the plant compartments were determined using PERMANOVA ($n = 198$). **g** PCoA of bacterial (upper panels) and fungal (lower panels) communities among the CSR-resistant and CSR-susceptible groups in the five compartments based on Bray–Curtis distances ($n = 198$)

separately collected samples from the four CSR-resistant and the four CSR-susceptible maize cultivars from five compartments: bulk soil (BS), rhizosphere soil (RS), root endosphere (RE), stem endosphere (SE), and grain endosphere (GE; Fig. 1b). We profiled the compositions of the bacterial and fungal communities based on sequencing of

the small ribosomal subunit (16S rRNA) gene fragments and internally transcribed spacer (ITS) sequences across the 8 cultivars, followed by clustering into operational taxonomic units (OTUs; 97% identity).

We obtained 12,824,344 rRNA and 15,788,680 ITS high-quality reads from 198 samples, ranging from 30,162 to 94,013 reads per sample, with an average of 72,255 reads per sample, representing 4624 bacterial and 1471 fungal OTUs. We employed a linear mixed model (LMM) to assess which major factors shape the Shannon diversity index (SDI) of maize microbiota. The LMM results suggested that compartment was the most important drivers of both bacterial ($P=2.2E-16$) and fungal ($P=2.2E-16$) SDI (Supplementary Table 3). Interestingly, we found that the interaction between CSR-resistance and compartments ($P=0.0087$) rather than CSR-resistance ($P=0.3418$) have a greater influence on bacterial SDI, indicating that the CSR resistance drive the bacterial SDI on in specific but not all the compartments. LMM results indicated that different cultivars have no effect on bacterial ($P=0.4447$) or fungal ($P=0.1405$) composition. This result was further confirmed by pairwise multilevel comparison using Adonis across the eight cultivars, which showed that most of pairwise cultivars within the same group (CSR-resistant or CSR-susceptible group) have no significant differences in microbiome composition (Supplementary Table 4).

We evaluated the assembly process of microbial communities, which is known to be strongly linked to the maintenance of plant health [25], based on the β-nearest taxon index (βNTI), which measures the mean phylogenetic distance between taxa of a community. We detected marked differences in βNTI in bacterial communities between CSR-resistant and CSR-susceptible sample pairs among the BS, RS, RE, and SE compartments. By contrast, we noticed no significant changes for fungal communities, suggesting that CSR resistance has a stronger influence on the assembly of bacterial rather than fungal microbiota (Fig. 1c, Supplementary Table 5, Wilcoxon rank sum test, $P<0.05$). The bacterial communities in soil (BS and RS) exhibited a different assembly compared to the internal compartments (RE, SE, and GE), whereas we detected no significant differences in fungal community assembly among the five compartments analyzed (Extended Data Fig. 1b).

Furthermore, the proportion of deterministic (HS homogeneous selection and VS variable selection, $|\beta NTI|>2$) and stochastic (DDH dispersal, drift, and homogenizing dispersal, $|\beta NTI|<2$) processes was different across compartments (Fig. 1d). The proportion of VS ($\beta NTI>2$) of bacterial communities increased in the RE and SE compartments of CSR-resistant cultivars relative to the other three compartments, indicating that the phylogenetic turnover and interaction among microorganisms were higher than expected. Neutral community model analysis showed that the dispersal ability and habitat niche breadth of bacterial communities decrease gradually from soil to internal compartments (Extended Data Fig. 1c, d). In the RS and RE compartments, the dispersal limitation on bacterial communities was higher in CSR-resistant cultivars than in CSR-susceptible samples, as reflected by the lower Nm values (an estimate of dispersal between communities). Collectively, these findings indicate that the root compartments of CSR-resistant cultivars undergo changes in its bacterial, rather than fungal, communities upon *F. graminearum* infection and that this compartment plays a prominent role in host plant resistance.

Distinct patterns of microbial diversity characterize different maize compartments

Assessments of Shannon diversity revealed significant differences between soil and plant compartments in both bacterial and fungal communities (Tukey's multiple comparisons test $P<0.05$, Fig. 1e, Supplementary Table 6). As a whole, the richness of bacterial and fungal species was lower in the maize internal compartments than in the soil, with GE displaying the least diversity. The SDI of bacterial communities showed no significant differences (Wilcoxon rank sum test, $P>0.05$) between CSR-resistant and CSR-susceptible groups among the five compartments. By contrast, the SDI of the fungal community were lower in the RE and SE niches of CSR-susceptible groups, suggesting that the microenvironment in these two compartments of CSR-susceptible cultivars is more susceptible to interference than CSR-resistant cultivars (Extended Data Fig. 1e).

Principal coordinates analysis (PCoA) based on Bray–Curtis dissimilarity clearly separated bacterial communities in the soil from the plant internal samples along the first principal coordinate (Fig. 1f, Supplementary Table 7). In parallel, we observed significant differences in the composition of bacterial communities in the three internal compartments along the second principal component. We noticed a similar positional variation pattern of fungal communities, as fungal communities in RE differed markedly from those in the other four compartments. Moreover, we identified significant differences in bacterial and fungal communities between CSR-resistant and CSR-susceptible samples in each compartment, except for bacteria in the GE (Fig. 1g, Supplementary Table 8). Overall, these results indicate that maize compartments and CSR-resistance have strong selective effects on the composition of microbiome communities.

Co-occurrence networks reveal stronger bacterial–fungal interactions in root-associated compartments of CSR-resistant maize cultivars

To investigate whether and how CSR resistance affects the complexity and stability of molecular ecological networks across the maize compartments, we constructed bacterial–fungal co-occurrence networks (Spearman's correlation coefficient (ρ) was > 0.9 and $P < 0.05$). We detected a clear shift in the interkingdom network patterns across the five maize compartments. The number of nodes (N), including both bacterial and fungal taxa, was lower in internal samples (RE, SE, and GE) than in soil samples (BS and RS; Fig. 2a, b). This finding was predictable, considering how soil tends to contain a greater diversity of microbes than the internal compartments of plants. Compared to CSR-susceptible cultivars, roots (RE and RS) of CSR-resistant samples had more nodes and edges, with higher connectivity and average degree. These more complex topological properties of bacterial–fungal networks in RE and RS represented stronger microbial interactions in root of CSR-resistant cultivars. We observed an opposite pattern in maize stems (SE) compared with roots that CSR-susceptible cultivars had the most edges, highest connectivity, and degree (Supplementary Table 9). In addition, the Bray–Curtis dissimilarity of root-associated networks (RS and RE) between CSR-resistant and CSR-susceptible groups was higher than that in the SE and GE compartments, indicating

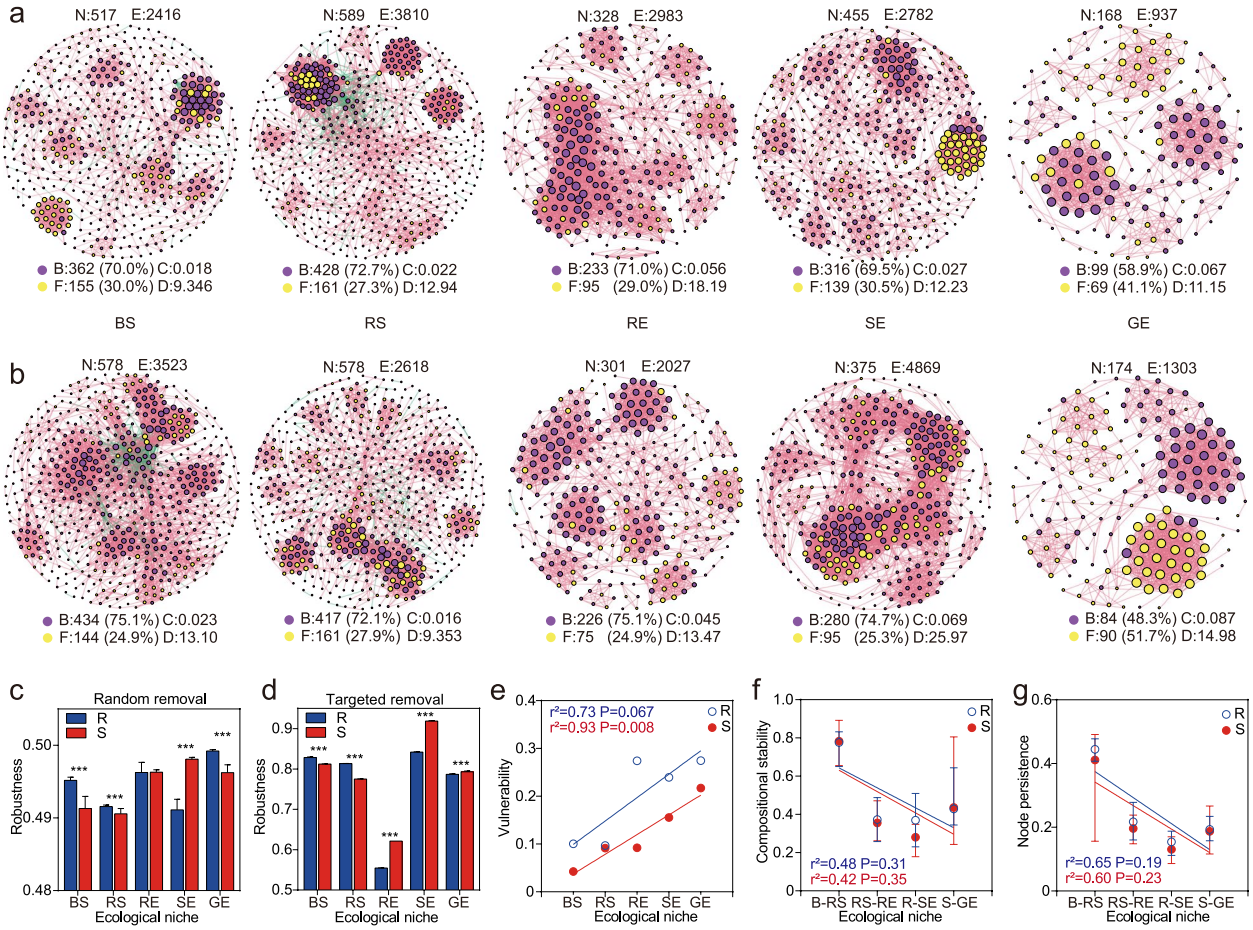

Fig. 2 Bacterial–fungal interkingdom networks in CSR-resistant and CSR-susceptible maize cultivars across the five compartments. **a**–**b** Bacterial–fungal interkingdom networks in CSR-resistant (**a**) and CSR-susceptible (**b**) maize cultivars. N, number of nodes; E, number of edges; B, number of bacterial OTUs; F, number of fungal OTUs; C, centralization betweenness; D, network diameter. **c** Robustness, as measured by randomly removing 50% of the taxa from each network. **d** Robustness, as measured by randomly removing 50% of the module hubs from each network. In c and d, each error bar corresponds to the 95% confidence interval of the mean. Significant differences between R and S groups were calculated using the Wilcoxon rank sum test (*** $P < 0.001$). **e** Vulnerability of the network, as measured based on maximum vulnerability across all nodes. **f** Compositional stability from every pair of adjacent compartments. **g** Node persistence from every pair of adjacent compartments. In e–g, the adjusted r^2 and *P*-values of linear regressions were determined by ANOVA

that microbes in root compartments had less stabilities than those in the stem and grain compartments (Supplementary Table 10). The interactive degree of *Fusarium* was specially extracted from each bacterial–fungal networks to investigate the pathogen-related interactions between CSR-resistant and CSR-susceptible cultivars. Results showed the drastic reduction in *Fusarium*-related interactive degree from RS to RE compartments in CSR-resistant cultivars, whereas the results of CSR-susceptible cultivars were the opposite (Extended Data Fig. 2a).

We calculated the robustness of each network by simulating species extinction, which reflected the intensity of interaction between bacteria and fungi. This analysis revealed marked divergence in robustness between CSR-resistant and CSR-susceptible groups by removal of either random taxa or targeted module hubs (Fig. 2c, d). Network vulnerability increased marginally, and the compositional stability and node persistence decreased along the bottom-up compartments in both the CSR-resistant and CSR-susceptible groups (Fig. 2e–g). These results suggest that compartments and CSR-resistance of the host plant greatly influence bacterial–fungal interactions.

Bacillus tends to be recruited across bottom-up compartments

To define the core microbiota associated with CSR-resistant plants, we comprehensively analyzed the taxonomic compositions and relative abundances of their bacterial and fungal communities. Microbial community analysis at the phylum level showed compartment specificity (Fig. 3a). The dominant bacterial phyla were Proteobacteria (63.23%), Acidobacteriota (13.10%), and Actinobacteriota (6.94%). Notably, Acidobacteriota mainly existed in

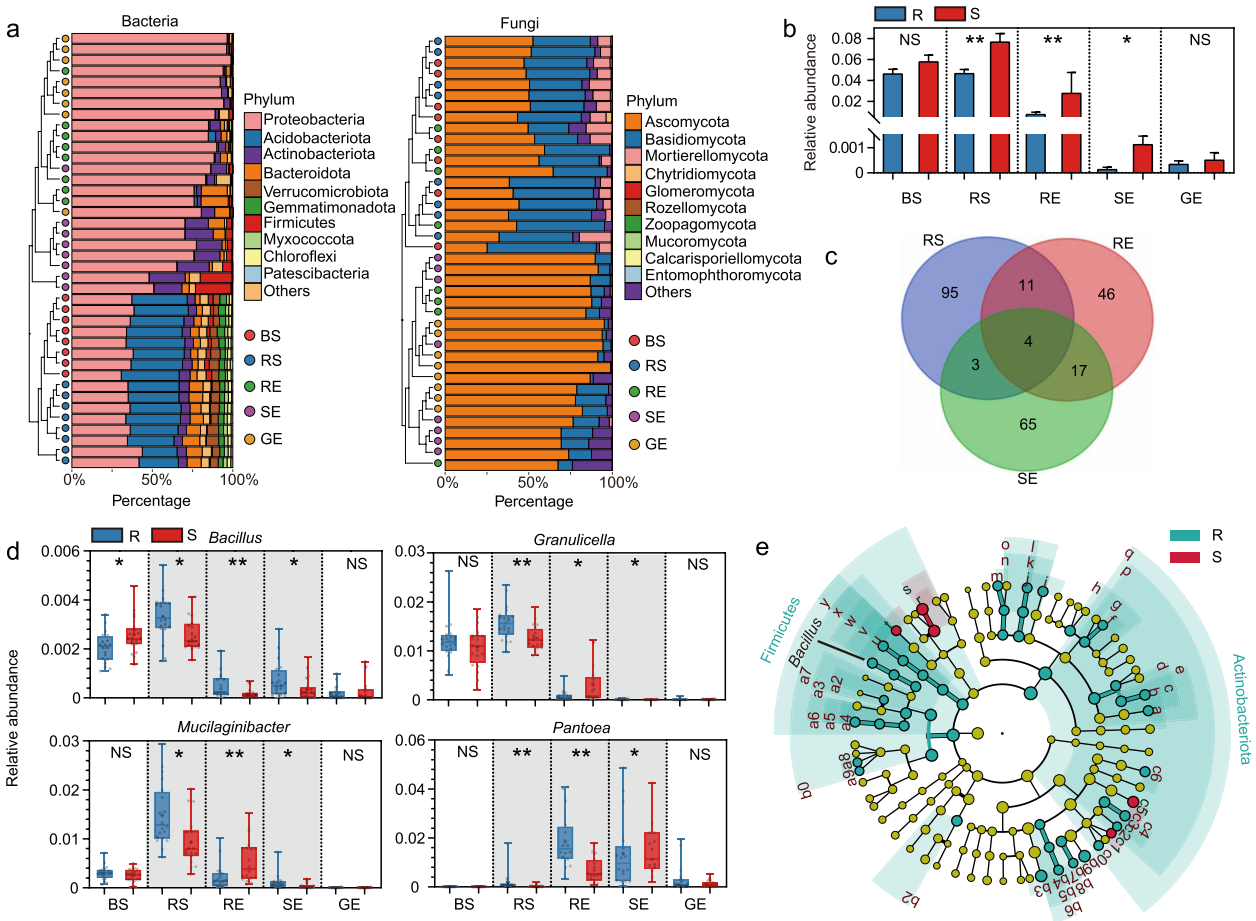

Fig. 3 Microbial community composition and candidate core disease-suppressive microbiota. **a** Relative abundance of the dominant bacterial and fungal phyla in the five compartments. **b** Relative abundance of *F. graminearum* in *ITS* rRNA sequencing data. **c** Number of shared and specific genera showing differences in abundance between the R and S groups (Wilcox test, $P < 0.05$). **d** Relative abundances of *Bacillus*, *Granulicella*, *Mucilaginibacter*, and *Pantoea* species among the five compartments. **e** Cladogram indicating the phylogenetic distribution of the bacterial lineages in the CSR-resistant (green) and CSR-susceptible (red) maize cultivars. Taxa with linear discriminant analysis (LDA) scores greater than 3 were selected as the biomarkers for the R and S groups

the two soil compartments, and the proportion of Actinobacteriota was higher in SE samples. A similar analysis of fungal communities showed that Ascomycota (65.29%) and Basidiomycota (24.93%) are the dominant phyla. Furthermore, measurement of the abundance of *F. graminearum* from ITS amplicon sequencing data showed that the proliferation of *F. graminearum* is significantly inhibited in the RS, RE, and SE compartments of CSR-resistant maize cultivars (Fig. 3b).

Core microbiome was defined as the taxa that appear in more than 80% samples (more than 158 of 198 samples in this study) [26]. A total of 19 bacterial and 16 fungal genera were geared to core taxa (Supplementary Table 11). We first identified the resistance-related taxa in CSR-resistant and CSR-susceptible groups through differential analysis, which demonstrated that four shared genera, i.e., *Bacillus* (belong to core taxa), *Granulicella*, *Mucilaginibacter*, and *Pantoea*, showed significant differences among the RS, RE, and SE compartments (Wilcoxon rank sum test, $P < 0.05$, Fig. 3c). Relative abundance measurements revealed that only *Bacillus* tended to be recruited that showed consistent higher abundance in the RS, RE, and SE compartments of CSR-resistant cultivars compared with the CSR-susceptible cultivars (Fig. 3d). Linear discriminant analysis effect size (LEfSe) with a logarithmic LDA > 2.5 further indicated that *Bacillus* can serve as a useful biomarker for CSR-resistant maize cultivars (Fig. 3e and Extended Data Fig. 2b). To identify the core fungal taxa of CSR-resistant maize plants, we investigated fungal communities using the same method. Two fungal taxa *Alternaria* and *Nigrospora* showed significant differences among the RS, RE, and SE compartments (Wilcoxon rank sum test, $P < 0.05$, Extended Data Fig. 2c). However, the abundance of *Nigrospora* was higher in RS and SE of CSR-susceptible than in CSR-resistant cultivars, and the abundance of *Alternaria* was higher in SE than in RS; neither of them showed the tendency to be recruited (Extended Data Fig. 2d). Considering the comprehensive research of *Trichoderma* for CSR suppression, the relative abundances of *Trichoderma* were specially investigated. No significant differences in relative abundance of *Trichoderma* were found across the five compartments (Extended Data Fig. 2d, Wilcoxon test, $P > 0.05$). Therefore, we selected *Bacillus* as a candidate core taxon for CSR-resistant cultivars and subjected it to a series of verification experiments.

The presence of *Bacillus* species enhances plant performance against *F. graminearum*

To explore the effects of the recruited bacteria on plant health, we purified 276 bacterial strains, accounting for 43% of all the OTUs with more than five reads in RS samples, from the rhizosphere soil of CSR-resistant cultivars using gradient dilution and streak plate techniques (Supplementary Table 12). These 276 isolates, including 62 *Bacillus* isolates, were categorized into 17 families based on 97% identity of 16S rRNA gene. In addition, we obtained 694 *Bacillus* isolates using the *Bacillus*-specific method. All the 756 *Bacillus* isolates from the two methods were clustered into 28 subgroups with 97% identity of the full length 16S rRNA gene within a subgroup which could be considered the same species. We randomly selected 44 isolates from the 28 subgroups for de novo genome sequencing and protein prediction. Based on these results, we assigned accurate taxonomies by reconstructing a neighbor-joining (NJ) phylogenetic tree from 4215 *Bacillus* genomes using the Composition Vector Tree (CVTree) Standalone Version, classifying the 44 isolates into 12 *Bacillus* subgroups (Fig. 4a).

We identified three models representing the antagonistic phenotype of all the isolates against *F. graminearum* in dual culture assays, which we characterized as follows: inhibition by pre-emption, inhibition by potential secretion of antimicrobial compounds, and no inhibition. Metagenomic mapping of 23 isolates showed an enrichment in CSR-resistant cultivars (marked by * in Fig. 4a,

(See figure on next page.)

Fig. 4 Dendrogram of the *Bacillus* isolates and suppressive activities against *F. graminearum*. **a** Dendrogram of 44 selected strains, reconstructed using the CVTree method. The three types of antagonistic phenotypes of 44 *Bacillus* isolates to *F. graminearum* in dual culture assays are marked by red, yellow, and gray circles, as shown in the key at the top. Gray shading in the strain names represents the same species adscription as shown on the right. Asterisks represent significantly higher abundance (two-tailed unpaired Wilcoxon rank sum test, *P*-value < 0.05) of the strain in CSR-resistant group determined by mapping metagenomic data to the genome of strain. **b** Overview of the growth status of maize seedlings (GZL455, CSR-resistant cultivar) at 2 weeks after treatment with sterile water as a control (CK), *F. graminearum* (Fg), Fg with SC-I, SC-II, or SC-III. **c** Mean incidence rates of maize seedlings (GZL455, CSR-resistant cultivar) at 2 weeks after *F. graminearum* inoculation. Values are means ± standard errors; different letters indicate significant differences (Wilcox test, $P < 0.05$, $n = 3$). **d** Upregulated and downregulated genes across the three SC treatments compared with the control groups treated with sterile water, with circle size corresponding to the FPKM values of genes. The DEGs were selected based on the criteria $|\log_2 FC| > 1$ and $P_{adj} < 0.05$. DEGs conforming to these criteria are indicated in red (up) and blue (down), whereas others are indicated in gray. **e**–**g** PCoA analysis among the groups based on Bray–Curtis dissimilarities using the top 500 genes (**e**), DEGs (**f**), and functionally related genes (**g**). **h** Tree map of the GSEA functional terms of maize roots treated with SC-III, with the size of boxes corresponding to the number of core genes related to each functional term. The NES values are shown under the functional pathway names. Numbers marked in red represent the high expressions of the most of the member genes corresponding to the enrichment items

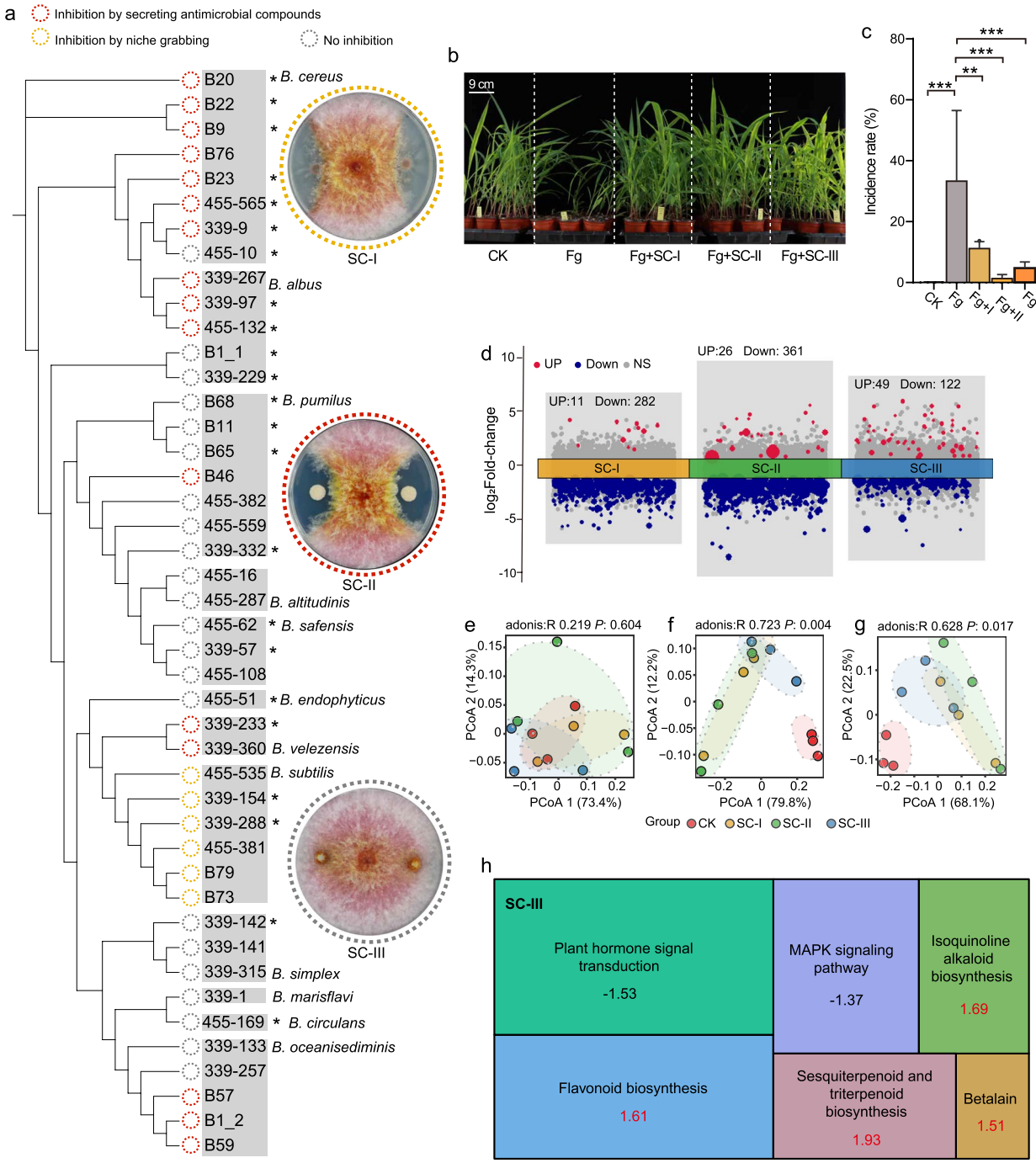

Fig. 4 (See legend on previous page.)

Wilcoxon rank sum test, $P < 0.05$) and represented two examples of pre-emption, nine examples of potential secretion of antimicrobial compounds, and 12 isolates with no inhibition.

We generated three types of synthetic communities (SCs) by randomly selecting and mixing three isolates from each model in equal-volume suspensions (SC-I, inhibition by pre-emption; SC-II, inhibition by potential secretion of antimicrobial compounds; SC-III, no inhibition). We investigated the disease suppression activity of these SCs against *F. graminearum* in greenhouse experiments using a CSR-resistant cultivar GZL455. Infected maize seedlings were characterized by hyphal radial growth at the base and the apparent yellowing of stems,

resulting in wilting within 2 weeks (Fig. 4b, Extended Data Fig. 3a). Pot experiments with three independent replications showed that SC-I, SC-II, and SC-III significantly decreased CSR incidence in maize seedlings at 2 weeks after *F. graminearum* inoculation (Fig. 4c). In addition, *F. graminearum* treatments reduced the rate of seedling emergence and root growth, while additional inoculation with *Bacillus* at the same time, especially with SC-II, restored these seedling phenotypes (Extended Data Fig. 3b–d).

To gain insight into the disease resistance mechanisms of the host plant based on their responses to pure *Bacillus* treatment, we investigated the transcriptomic changes of the CSR-resistant cultivar GZL455 in maize roots treated with these three types of SCs and sterile water as the control group. We obtained 534,236,556 high-quality reads, with an average of 44,519,713 reads per sample and a 94.6% mapping rate to the maize reference genome (B73-NAM-5.0). Compared to the control groups treated with sterile water, we identified 293, 387, and 171 differentially expressed genes (DEGs, $|\log_2(\text{fold-change})| > 1$, $P_{adj} < 0.05$) in maize roots treated with SC-I, SC-II, and SC-III, respectively (Fig. 4d). PCoA based on an expression matrix of all genes showed that SC treatment did not greatly alter gene expression in maize roots (Fig. 4e), whereas PCoA based on DEGs (Fig. 4f) and functionally related genes (Fig. 4g) showed that SC-I and SC-II had similar effects on maize that were different from those observed for SC-III.

Gene set enrichment analysis in response to treatment with each SC revealed similar enrichment among DEGs for functional terms such as mitogen-activated protein kinase (MAPK) signaling and plant hormone signal transduction (Fig. 4h, Extended Data Fig. 4a, b, Supplementary Table 13). Notably, inoculation with any of the three SCs resulted in lower expression of *WRKY33*-homologous genes, which facilitate defense-related gene induction (Fig. 5a).

We were most interested in the SC-III-specific functional pathway, since SC-III had no inhibitory effect on *F. graminearum* but significantly decreased the incidence of CSR. Furthermore, SC-III, rather than SC-I or SC-II, specifically affects the transcriptional expression of maize genes related to sesquiterpenoid, isoquinoline alkaloid, and betalain biosynthesis, as reflected by the normalized enrichment scores (NESs); these compounds are widely considered to be antibacterial metabolites (Fig. 4h). Both *terpene synthase 6* (*TPS6*) and *tyrosine decarboxylase 1* (*TYDC1*), which participate in the above pathways, were upregulated by treatment with SC-III. The functional terms phenylalanine and tyrosine metabolites, which are biosynthetic precursors of isoquinoline alkaloids, were also enriched by treatment with SC-III (Supplementary Table 13). We validated the expression patterns of the abovementioned genes by RT-qPCR analysis (Fig. 5b and Extended Data Fig. 4c).

Isoquinoline alkaloids are enriched in CSR-resistant cultivars and suppress CSR

To investigate the biochemical composition of the root microenvironments, we determined the identities of metabolites in RS and RE samples collected from CSR-resistant and CSR-susceptible cultivars treated with *F. graminearum* in 2021 by liquid chromatography–tandem mass spectrometry (LC–MS/MS). We detected an average of 1558 metabolites across all samples (Supplementary Tables 14–15). PCoA based on Bray–Curtis distance matrices revealed significant differences in both RS and RE metabolites between CSR-resistant and CSR-susceptible samples ($P = 0.008$, PERMANOVA by Adonis, Fig. 5c). We identified 947 significantly different metabolites in RE samples and 124 in RS samples ($|\log_2 FC| > 1$, $P < 0.05$), demonstrating the presence of distinct chemical microenvironments in these two compartments.

Consistent with the transcriptomic data (Fig. 4h), berberine (a natural isoquinoline alkaloid) and its isoquinoline precursor were enriched in the RE compartment rather than the RS compartment. The biosynthetic precursor L-phenylalanine appeared to be depleted from CSR-resistant samples (Fig. 5d, Extended Data Fig. 4d). Importantly, L-dopa and tyramine, members of the berberine biosynthesis pathway that are substrates used by TYDC1 to synthesize dopamine, were enriched in RE samples (Extended Data Fig. 4d). The antagonistic activities of berberine against *F. graminearum* were demonstrated in vitro. In potato dextrose agar (PDA) plate assays, *F. graminearum* growth was reduced as the concentration of berberine increased, with growth diameters decreasing by 37%, 52%, 54%, and 58% in the presence of 5, 25, 50, and 100 μg/mL berberine, respectively (Fig. 5e and Extended Data Fig. 4e). Finally, pre-treatment of seed coats (GZL200) with berberine significantly reduced CSR disease severity (Fig. 5f). Together, these results at the transcriptional and metabolic levels indicate that SC-III treatment triggers disease-suppressive activity in the RE compartment by inducing the accumulation of antifungal metabolites.

Discussion

Host-associated bacteria account for approximately 70 to 90% of total soil microorganisms and harbor 100-fold more functional genes than the host [27], making them worthy of being the optimal choice to form holobionts with their host. The phenotype of a plant depends primarily on the integration of the plant's genotype, the associated microbiota, and the field microclimate [28,

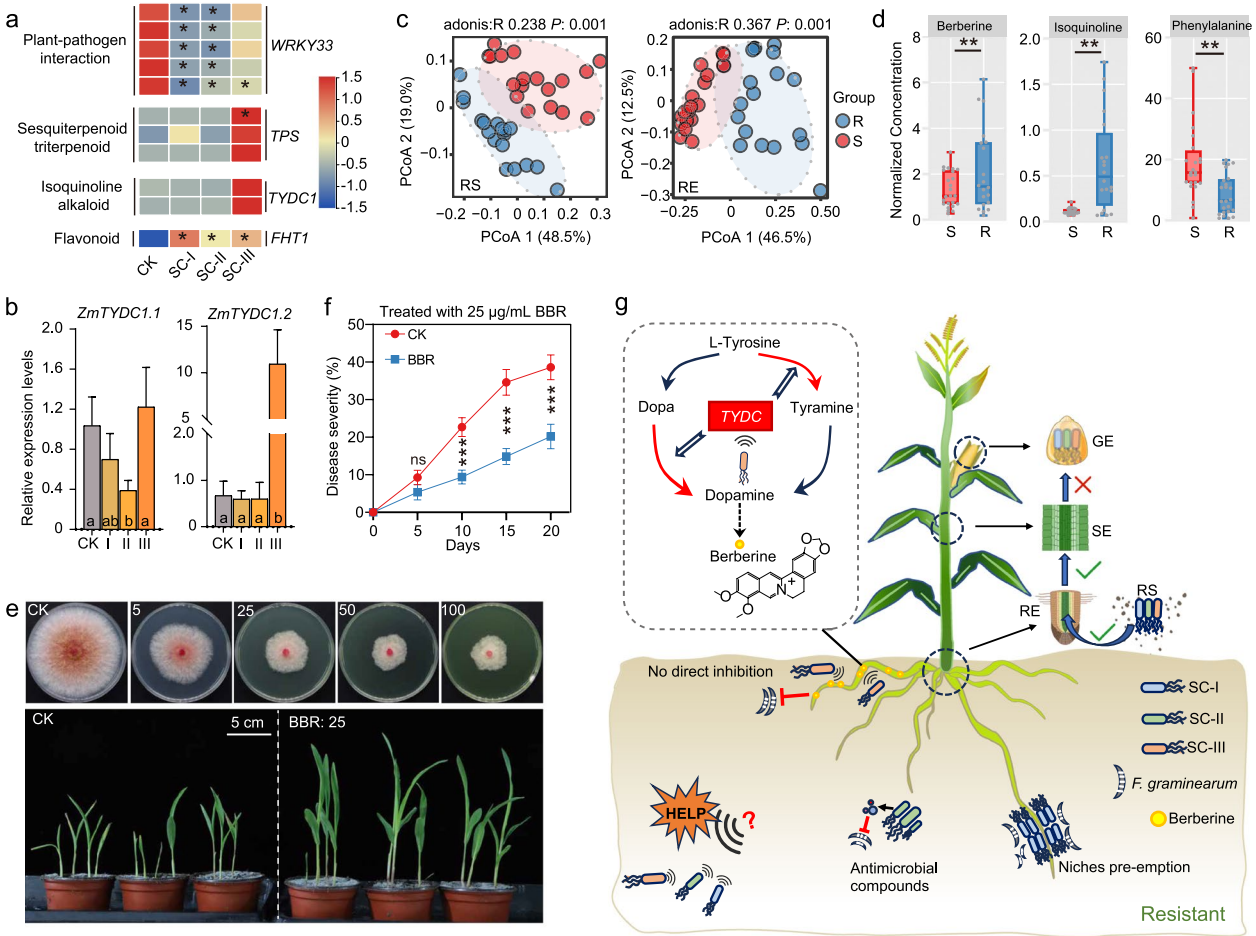

Fig. 5 Isoquinoline alkaloids are involved in CSR disease suppression. **a** Heatmap showing the expression trends of genes involved in the selected functional pathways. * represents a significant difference ($P < 0.05$) compared to the CK group. **b** Relative expression levels of maize *TYDC1*, as determined by RT-qPCR. The values are means ± SDs ($n = 3$). Significant differences ($P < 0.05$) were calculated by one-way ANOVA and are shown with different lowercase letters. **c** PCoA based on Bray–Curtis distance matrices of maize RS (left) and RE (right) metabolites in CSR-resistant and CSR-susceptible groups. **d** Normalized concentrations of berberine (BBR), isoquinoline, and L-phenylalanine in RE compartment, as determined by LC–MS/MS. **e** Inhibitory effects of 5% (v/v) DMSO (CK) and 5, 25, 50, and 100 μg/mL berberine on mycelial growth (upper panels) and 25 μg/mL berberine on disease severity (lower panels). **f** Disease severity (as mean ± SD) of maize seedlings treated with Fg (10^5 spores/mL, CK) and additional berberine (25 μg/mL, BBR). **g** Proposed model of the microbial assembly across different CSR resistance and compartments challenged with *Fusarium* CSR. Maize cultivars resistant to CSR reshape the microbiota and recruit three types of *Bacillus* species (SC-I, inhibition by pre-emption; SC-II, inhibition by potential secretion of antimicrobial compounds; and SC-III, no direct inhibition but induction of berberine biosynthesis by the host), conferring benefits in disease suppression. SC-III facilitates berberine biosynthesis by inducing the expression of *TYDC*, encoding an enzyme that catalyzes the production of dopamine from L-dopa and tyramine. These beneficial *Bacillus* can be recruited from the rhizosphere soil (RS) compartment via the root endosphere (RE) compartment to the stem endosphere (RE) compartment, but not to the grain endosphere (GE) compartments

29]. Accumulating evidence suggests that plants actively reshape specific communities of microorganisms to alter their phenotypes, promote growth, and even inhibit disease occurrence [30]. Our 16S rRNA gene analysis demonstrated that both the maize compartments and the host CSR-resistance significantly shape the ecological assembly processes of bacterial, rather than fungal, communities. This plasticity in bacterial communities was further verified by diversity analysis. Although our observations do not align with the results of many studies that show that fungal *Trichoderma* species suppress CSR symptoms [31], we and others have witnessed an important bacterial community response to CSR [32, 33].

The dispersal ability and habitat niche breadth of bacterial communities decreased gradually from the soil to internal compartments, indicating that selection pressure increases during the movement of microbes from belowground to aboveground compartments. The plant

immune system and associated biochemical barriers are thought to result in strong selective pressure on the microbiota inhabiting inner plant tissues [34]. Our neutral community model analysis further indicated that RS and RE compartments in CSR-resistant, rather than CSR-susceptible, maize cultivars provide stronger dispersal limitation and selection pressure. These findings underscore the potential role of maize roots as a physical barrier and selection driver in shaping bacterial communities. The precipitous decline in microbial diversity from soil to internal compartments and the clearly separated communities revealed by PCoA also support the role of maize roots in shaping their bacterial communities. In addition, our study demonstrated that the diversity of bacterial communities was much lower in the reproductive organ (grain) than in vegetative organs (root or stem) and that the assembly process of bacterial communities in the grain was not affected by the resistance genotype of the host plant. Thus, the less-pronounced effect of CSR-resistance and compartments on microorganisms within grains can be explained by a life history tradeoff strategy that ensures the survival of the next generation of the host plant at the expense of investing in the susceptible individual in the current generation [18, 35].

Microbiota do not live in isolation, instead forming complex interactions with living organisms and nonliving environments through the exchange of matter, energy, and signal, as shown by networks with species as nodes and associations as edges [36]. The co-occurrence of species is thought to be mainly driven by three ecological responses: biological interactions, environmental filtration, and diffusion restriction. Among these responses, biological interactions may be the main driving force for the overall network [37, 38]. In this study, the bacterial–fungal interkingdom networks in soil showed richer compositions and more complex interactions than those in internal compartments, which is in agreement with earlier studies [39]. Importantly, the root-related compartments (RS), but not the other compartments, showed stronger interactions among bacterial–fungal interkingdom networks in CSR-resistant maize than in CSR-susceptible maize. Thus, we suggest that roots are the key regions where CSR-resistant maize shapes the bacterial community and thereby promotes disease resistance.

Fusarium species secrete mycotoxins that cause plant diseases such as stem rot, Fusarium wilt, and scab and ear rot, resulting in significant losses in crop production [40]. In contrast to chemical control methods, the use of biological control agents provides a safe, effective, sustainable means of controlling plant diseases caused by *Fusarium*. Using multiple bioinformatics methods, we identified *Bacillus* as the core microbiota of CSR-resistant cultivars; our greenhouse experiments further confirmed that *Bacillus* treatment significantly inhibits CSR. These findings are consistent with those of studies showing that *Bacillus* can antagonize *Fusarium* infection in multiple ways: niche competition, the production of antibacterial substances, and the induction of plant systemic resistance [41, 42].

We showed that *B. cereus* and *B. albus* antagonize *F. graminearum* by secreting antimicrobial compounds (Fig. 4a). A previous study identified hentriacontane and butylphenol as key antifungal volatile organic compounds produced by *B. cereus* that improve the resistance of tomato (*Solanum lycopersicum*) plants to Fusarium wilt [43]. Although there is no direct evidence in previous researches that *B. albus* inhibits pathogen activity, *B. albus* was reported to produce cellulase, which acts as an antifungal protein capable of rupturing pathogenic cell walls [44]. In the current study, *B. subtilis* demonstrated strong space competitiveness and monopolized nutritional resources, which is consistent with previous findings [42, 45].

Surprisingly, macroscopic disease was suppressed when maize seedlings were treated with SC-III which showed no inhibitions to *F. graminearum* in dual culture assays. Maize root transcriptome sequencing showed that SC-III specifically facilitated the enrichment of molecules involved in sesquiterpenoid, isoquinoline alkaloid, and betalain biosynthesis. Although the plant growth–promoting effects of SC-III was not verified in this study, these *Bacillus* species that belong to SC-III were reported to improve host performance by increasing the emergence of lateral roots in pea (*Pisum sativum*; *B. simplex*), shoot dry mass in chickpea (*Cicer arietinum*; *B. pumilus*), root length in *Brassica juncea* (*B. safensis*) and germination index in rice (*Oryza sativa*; *B. altitudinis*) [46–49]. Therefore, we suggest that these strains may induce disease resistance by beneficially interacting with the host, including indirectly enhancing plant performance and directly inducing the alkaloid synthesis.

The two-way production and perception of secretions of both microbiota and plant host is a key mechanism through which plants interact with their microbiota [50]. Under biotic and abiotic stress, plant roots secrete specific exudates to shape rhizospheric microbiomes, whereas microbiomes modulate the soil environment by reprogramming root exudation profiles [51, 52]. Acknowledging the crucial effect of roots on shaping microenvironments, we further explored the specific compositions and differentiation of these root exudates. We demonstrated that the metabolic profiles of CSR-resistant and -susceptible maize cultivars are distinct. This observation is consistent with the expectation that complex root systems and wide genomic diversity of maize result in major physiological differences [53].

Distinct maize genotypes have been shown to differ in their enrichment of specific bacterial taxa [53]. In line with the results of transcriptome functional enrichment, isoquinoline alkaloid pathways, together with the isoquinoline precursor, were enriched in the RE compartment of CSR-resistant cultivars when treated with SC-III, and they exhibited both in vitro antagonistic activities and in vivo disease suppression effects. This finding is consistent with the previous observations that isoquinoline alkaloid biosynthesis was significantly upregulated in maize seedlings infected with rice black streaked dwarf virus based on transcriptomic data and with *Fusarium verticillioides* based on metabolic profiles [54, 55]. However, these studies did not focus on the associated changes in the microbiota.

A previous study of the microbiota–host interaction in fava bean (*Vicia faba*) demonstrated that the antifungal peptide P852 from *Bacillus* fermentation broth could control Fusarium wilt by promoting the activities of antioxidant enzymes and enhancing isoquinoline alkaloid biosynthesis [56]. Although a clear link between *Bacillus* treatment and isoquinoline alkaloid biosynthesis was revealed by these findings and the current results, we cannot exclude the possibility that other factors, such as WRKY33-related induction of CSR-resistance, contribute to disease suppression. Considering that SC-I inhibited *WRKY33* expression but resulted in weaker disease suppression effects compared to SC-III, we suggest that isoquinoline alkaloids play important roles in the resistance of maize cultivars to CSR. It will be interesting to examine whether CSR-resistant maize plants secrete isoquinoline alkaloids, which could potentially inhibit the colonization and invasion of a wider range of pathogens. Together, these findings highlight the important role of *Bacillus* species as a key microbiota for suppressing *Fusarium*-induced diseases through multiple mechanisms, including the direct pathogen antagonism and the induction of alkaloid biosynthesis by the host (Fig. 5g).

Conclusions

Using multi-omics analyses and experimental validation, we showed that CSR-resistant host plants govern the assembly of distinct, beneficial microbial communities in their internal compartments. We also demonstrated that *Bacillus* species are core components of the microbiota recruited by CSR-resistant maize cultivars in the RS, RE, and SE compartments. In contrast to fungal microbiota, which showed little effect in preventing CSR, several *Bacillus* species decreased the incidence and symptoms of CSR via the secretion of antimicrobial compounds and the induction of host alkaloid biosynthesis. Although treatment with the SC-III suspension did not inhibit *F. graminearum* in vitro, it specifically induced endogenous isoquinoline alkaloid biosynthesis in vivo in the RE compartment. Overall, these findings improve our understanding of the roles of *Bacillus* as the core microbiotas in plant responses to *Fusarium* challenge and lay the foundation for preventing and treating *Fusarium*-induced disease.

Methods

Experimental design and sampling

The experiments were conducted in Gongzhuling City (43° 53′ N, 124° 82′ E), Jilin Province, northeastern China, a site that is considered to be one of the three golden corn belts. The site has a temperate continental monsoon climate with an annual average temperature of 5.6 °C, average annual precipitation of 595 mm, and a frost-free period of 144 days. Forty maize (*Zea mays*) cultivars (Supplementary Table 1) from a 527 association mapping panel [57] were planted in natural plots and disease nursery plots constructed for disease evaluation in early May 2020 and 2021. For the disease nursery plots, the inoculum preparation was firstly performed by incubating the mycelium of *Fusarium graminearum* from PDA medium into high-temperature-disinfected maize kernels in conical flask for 2 weeks. Then, 20 g of the maize kernels infected with *F. graminearum* were inoculated in the rhizosphere zone of each maize plants at the vegetative 6 (V6) stage by digging up the topsoil without damaging the roots. Maize plants at the reproductive 3 (R3) stage that showed no watery spots on their stems or brown withered stems were defined as healthy; plants with watery spots on their stems and hollow stems with brown xylem were classified as diseased. Surveys for the incidence of CSR (percentage of the total number of plants showing disease symptoms) were performed at the end of September 2020 and 2021. Maize cultivars that lacked CSR symptoms for two consecutive years were defined as CSR-resistant; cultivars with an incidence of CSR greater than 30% for two consecutive years were defined as CSR-susceptible.

To validate the participation of soil microbiome in resistance to CSR, natural field 0 ~ 25 cm topsoil was collected from Gongzhuling city and immediately transferred to the greenhouse for pot experiments. Before using, the topsoil was sieved by the screen with a diameter of 2 mm to remove stones and plant debris. The sieved soil was sterilized at 121 °C for 5 h in the sealable bag which kept the moisture constant. Four surface-disinfected maize seeds (GZL54, GZL185, GZL339, and GZL455) were planted into a plot with 300 g natural soil or a plot with equal volume of sterile soil. Every 7 days, 10 mL *F. graminearum* suspension in sterile water (10^5 spores/mL) were inoculated into the base of each maize seedling. Each treatment contained more than 45

maize seedlings and experiments were replicated three times. Three weeks after emergence when the pathogenetic seedlings withered and died, the disease index was recorded by diseased plants accounted for the proportion of total seedling number. Wilcox rank sum test was employed to test the statistical significance in R v4.1.0.

Four CSR-susceptible and four CSR-resistant maize cultivars were selected in October 2020 and again in October 2021 for experimentation. The experiments were conducted under the abovementioned field conditions. After soil inoculation with *F. graminearum* at the V6 stage, five maize compartments were individually sampled from each maize plant at R3 stage: bulk soil (BS), rhizosphere (RS), root endosphere (RE), stem endosphere (SE), and grain endosphere (GE), as illustrated in Fig. 1b. Bulk soil samples were collected by manually shaking uprooted plants; soil that loosely adhered to the roots was sampled as bulk soil. Rhizosphere soil was collected after manually removing the loose soil which leaved approximately 1 mm of soil on the roots. The roots were placed in a sterile 50-mL tube containing 30 mL of PBS and then vibrated for 15 s at maximum speed. Then, the large sediment and plant tissue were filtered by a 50-mL tube with a 100-μm nylon mesh cell strainer. Firm pellets containing the rhizosphere sample were obtained by centrifuging the turbid filtrate at 10,000 g for 5 min. All collected maize tissues were transported to the laboratory in a dry ice box and stored at − 80 °C for subsequent experiments.

DNA extraction and amplicon sequencing

For surface disinfection, a minimum of 5 g of roots, stems, or seeds was rinsed with 70% (v/v) ethanol for 5 min and then with 6% (w/v) sodium hypochlorite solution for 10 min, followed by three rinses in sterile water for 15 min. The treated tissues were ground into a powder in liquid nitrogen using a sterile mortar and pestle. Total DNA from 0.5 g bulk soil and rhizosphere soil, 0.2 g surface-disinfected root, stem, and seed were extracted using a FastDNA SPIN Kit for Soil (MP Biomedicals, Solon, USA) following the manufacturer's instructions. The V5–V7 region (799F: 5′-AACMGGATTAGATACCCKG-3′ and1193R: 5′-ACGTCATCCCCACCTTCC-3′) of the small ribosomal subunit (16S rRNA) gene and the fungal *ITS1* region (ITS1F: 5′-CTTGGTCATTTAGAGGAAGTAA-3′ and TIS1R: 5′-GCTGCGTTCTTCATCGATGC-3′) in the internal tissues were amplified. The V3–V4 region (341F: 5′-CCTAYGGGRBGCASCAG-3′ and 806R: 5′-GGACTACNNGGGTATCTAAT-3′) of the bacterial 16S rRNA gene and the fungal *ITS1* region (ITS1F/TIS1R) in the bulk soil and rhizosphere soil samples were also amplified. All PCR reactions were carried out with 15 μL of Phusion® High-Fidelity PCR Master Mix (New England Biolabs); 2 μM of forward and reverse primers; and about 10 ng template DNA. Thermal cycling consisted of initial denaturation at 98℃ for 1 min, followed by 30 cycles of denaturation at 98℃ for 10 s, annealing at 50℃ for 30 s, and elongation at 72℃ for 30 s; finally 72℃ for 5 min. Mix same volume of 1XTAE buffer with PCR products and operate electrophoresis on 2% agarose gel for detection. PCR products were mixed in equidensity ratios. Then, mixture PCR products was purified with Universal DNA (TianGen, China). Sequencing libraries were generated using NEB Next® Ultra DNA Library Prep Kit (Illumina, USA) following manufacturer's recommendations and index codes were added. The library quality was assessed on the Agilent 5400 (Agilent Technologies Co, Ltd., USA). The amplicon libraries were sequenced using the Illumina NovaSeq PE250 platform (Wekemo Tech Group Co., Ltd., Shenzhen, China) with a paired-end protocol.

Bioinformatic analysis of amplicon sequencing data

QIIME v1.9 [58] and USEARCH v10 [59] were used to process the bacterial 16S rRNA gene and fungal *ITS* sequences. Briefly, FastQC v0.11.5 [60] was used to assess read quality. Low-quality reads with scores below Q30 were trimmed in pairs using Trimmomatic v0.39 [61]. The corrected reads were merged into a single read and selected at 97% identity (operational taxonomic units, OTUs). The SILVA v138.1 [62] and UNITE v8.2 [63] databases were used to classify the sequences as bacterial or fungal. The OTU tables of bacteria and fungi were normalized according to the cumulative sum scaling (CSS) method with the script normalize_table.py in QIIME for alpha-diversity estimates. The cumulative sum scaling (CSS) normalization method was used for bacterial and fungal β-diversity analyses using beta_diversity.py. The OTUs present in all samples were defined as core taxa.

Principal coordinates analysis (PCoA) was performed using the Vegan v2.6.4 and Tidyverse v2.0.0 packages of R v 4.1.0 [64] based on the relative abundance of each OTU. Gehpi v0.9.2 [65] was used to produce the visualizations of the bacterial–fungal interkingdom networks (Spearman $|\rho| > 0.7$ and $P < 0.01$) following a previously described method [66]. To explore the degree of deviation of the co-accordance networks, dissimilarity was calculated using a previously described formula [67]. In addition, weighted robustness, vulnerability, compositional stability, and node persistence were evaluated using the ggClusterNet v0.1.0 package in R. A random-forest machine-learning model was established using a tenfold cross-validation error curve in the random Forest v4.7.1.1 package in R. Linear discriminant analysis effect size with permutational multivariate analysis of variance (PERMANOVA) based on 9999 permutations was

employed to identify the key families in the CSR-resistant and CSR-susceptible groups using the Vegan package in R. Beta nearest taxon index (βNTI) was calculated based on the OTU matrix using the ape, ICAMP v1.5.12, picante, and NST v3.1.10 packages in R. A neutral community model was conducted to estimate the effects of stochasticity on community assembly, in which the best fit between the frequency of OTU occurrence was generated by applying a nonlinear least-squares method [68].

Validating the role of the soil microbiome in CSR-resistant cultivars

Topsoil (0–25 cm) was collected from the large-scale sampled field, which had no history of maize cultivation. To obtain soil extracts, 1 g of soil was suspended in 9 mL sterile water, and the large soil particles were removed by filtration through Whatman 42 filter paper with 0.25 μm pore diameter. The CSR-resistant cultivar GZL185 was planted in sterile substrate that had been incubated for 2 weeks with soil extracts. After 5 days of growth, the root zone of each maize seedling was irrigated with 10 mL of a spore suspension of *F. graminearum* in sterile water (isolated from diseased maize in the field in Gongzhuling City) at a concentration of 2×10^5 spores/mL. Three weeks after *F. graminearum* inoculation, disease incidence, defined as the percentage of diseased seedlings relative to the total number of seedlings, was monitored.

Metagenomic sequencing and data mining

A total of 42 DNA samples (3 CSR-resistant and 3 CSR-susceptible cultivars with 3 replicates in 2020, 4 CSR-resistant and 4 CSR-susceptible cultivars with 3 replicates in 2021) were selected for metagenomic sequencing. Sequencing library was generated using NEBNext® UltraTM DNA Library Prep Kit for Illumina (NEB, USA, Catalog#:E7370L) following manufacturer's recommendations and index codes were added to each sample. Briefly, genomic DNA sample was fragmented by sonication to a size of 350 bp. Then, DNA fragments were endpolished, A-tailed, and ligated with the full-length adapter for Illumina sequencing, followed by further PCR amplification. After PCR products were purified by AMPure XP system (Beverly, USA). Subsequently, library quality was assessed on the Agilent 5400 system (Agilent, USA) and quantified by QPCR (1.5 nM). The qualified libraries were pooled and sequenced on Illumina NovaSeq 6000 (Wekemo Tech Group Co., Ltd., Shenzhen, China) with a paired-end protocol according to effective library concentration and data amount required. After removing the adaptor and low-quality sequences with Trimmomatic v0.39, Bowtie2 v2.1.0 was used to eliminate the host-derived sequences by mapping the clean data to the maize genome (B73 RedGen_v4 from maize GDB). The high-quality reads were assembled using Megahit v1.2.9 [69] with the parameter meta-large, predicted based on contigs using Prodigal (reads shorter than 300 bp were remove, v2.6.3) [70], and were clustered at 0.95 similarity threshold using CD-hit v4.6.2 [71] to generate non-redundant gene catalog.

Root collection and LC–MS/MS analysis

RS and RE samples from the field maize treated with *F. graminearum* in 2021 were selected for LC–MS/MS analysis. First, 10 mg portions of soil samples was transferred into centrifuge tubes containing 500 μL ddH_2O (precooled to 4 °C) and vortexed for 60 s. After the addition of 1000 μL methanol (prechilled to − 20 °C), the tubes were placed into an ultrasound machine at room temperature for 10 min and incubated on ice for 30 min. The samples were centrifuged for 10 min at 16,000 g at 4 °C, after which 1.2 mL of supernatant was transferred into a new centrifuge tube. Following vacuum concentration, the samples were dissolved in 40 μL 2-chlorobenzalanine (4 ppm) in a methanol:water solution (1:1, v/v, 4 °C). Following filtration through a 0.22-μm membrane, the samples were ready for LC–MS/MS detection.

To monitor deviations in the analytical results from these pooled mixtures and to compare them to the errors caused by the analytical instrument itself, 20 μL aliquots were removed from each prepared sample and mixed. LC analyses were performed on a Thermo Ultimate 3000 system equipped with an ACQUITY UPLC® HSS T3 (150 × 2.1 mm, 1.8 μm, Waters) column maintained at 40 °C. The temperature of the autosampler was set to 8 °C. Gradient elution of analytes was carried out using 0.1% (v/v) formic acid in acetonitrile (C) and 0.1% (v/v) formic acid in water (D) or acetonitrile (A) and 5 mM ammonium formate in water (B) at a flow rate of 0.25 mL/min. Each sample (2 μL) was injected following equilibration. An increasing linear gradient of solvent B (all v/v) was used as follows: 0–1 min, 2% A/C; 1–9 min, 2–50% A/C; 9–12 min, 50–98% A/C; 12–13.5 min, 98% A/C; 13.5–14 min, 98–2% A/C; 14–20 min, 2% A/C-positive mode (14–17 min, 2% A/C, negative mode). The ESI-MSn experiments were performed using a Thermo Q Exactive Focus mass spectrometer with spray voltages of 3.8 kV and − 2.5 kV in positive and negative modes, respectively. Sheath gas and auxiliary gas were set to 45 and 15 arbitrary units, respectively. The capillary temperature was 325 °C. The Orbitrap analyzer scanned over a mass/charge range of 81–1000 for full scans at a mass resolution of 70,000. Data-dependent acquisition (DDA) MS/MS experiments were performed with HCD scan. The normalized collision energy was 30 eV. Dynamic exclusion was implemented to remove unnecessary information in the MS/MS spectra.

The raw data were converted to MzXML files using Proteowizard v3.0.8789 [72]. Peaks identification, filtration, alignment, and grouping were performed with R package XCMS v3.16.1. Annotation of adducts and calculating hypothetical masses for the group were performed with R package CAMERA v3.1–5. In the extracted ion features, only the variables with > 50% of nonzero measurement values in at least one group were kept. QC quality control, batch effects removal, and normalization were performed with R package MetaboAnalystR v3.2. Briefly, the abundance of all features was divided by the median abundance of that sample to make the data close to a normal distribution. PCoA with Bray–Curtis distances was performed using R package vegan, and a pairwise Adonis test and PERMANOVA (999 permutations) were performed using R package amplicon.

Isolation and culture of bacterial strains from CSR-resistant samples

Methods for isolating and cultivating the bacteria in this study were described by Yang Bai et al. [29]. Briefly, tenfold serial dilutions of the rhizosphere microbiota sample in tryptic soy broth (TSB, Difco Laboratories Inc., Detroit, MI, USA) were prepared in 96-well cell culture plates. The plates were chosen in such a way that < 30% of the wells showed visible bacterial growth after an incubation period. Purified bacterial isolates were obtained by continuous streaking on solid Luria–Bertani (LB) medium, and identities were confirmed by 16S rRNA gene sequencing. All purified bacterial isolates were then placed in 50% (v/v) glycerol for storage at − 80 °C for subsequent experiments.

The *Bacillus* strains were further isolated. Briefly, 10 g of soil was placed into 90 mL sterile water, and a 10^{-5} soil suspension was prepared by successive tenfold dilutions in sterile water. The suspension was incubated in a water bath at 80 °C for 30 min to kill the non-endospore-forming bacteria. A 0.1-mL aliquot of the diluted suspension was spread onto plates containing LB medium and incubated for 12 h at 37 °C. Single isolates were preliminarily classified according to the identity of full-length 16S rRNA genes mapping to the NCBI rRNA/ITS database, and the single colonies were purified. The surviving strains were then stored in a refrigerator at 4 °C for future use.

Genomic sequencing of *Bacillus* isolates

To obtain accurate classification information, the genomes of 44 isolates were sequenced. Briefly, genomic DNA was extracted from each isolate using a Bacterial Genomic DNA Extraction Kit (Qiagen), and a sequencing library was generated using a VAHTS Universal DNA Library Prep Kit for Illumina (Vazyme, ND604) following the manufacturer's recommendations. The library preparations were sequenced on the Illumina NovaSeq 6000 platform with the 150-bp paired-end module.

After obtaining the raw data, the raw reads were filtered by removing reads containing adaptor, poly-N, and low-quality reads (more than 50% of bases with Q < 10). SPAdes v3.15.5 [73] was used to perform genome assembly with gradient k values (21, 33, 55, 77, 99, and 127), and annotation was accomplished using Prokka v1.13 [74]. To obtain taxonomy information about the isolates, a neighbor-joining (NJ) phylogenetic tree was reconstructed based on the amino acid sequences of 4215 genomes of *Bacillus* species using the CVTree Standalone Version with k-string = 6 [75]. The abundance of these isolates in the rhizosphere was determined by mapping the metagenomic data to these genomes using Bowtie2 v2.1.0 with parameter very sensitive.

Measuring in vitro antagonistic activities of bacteria against *F. graminearum*

The antagonistic activities of bacteria against *F. graminearum* were measured by in vitro dual culture assays on potato dextrose agar (PDA, Difco) solid medium. Petri dishes containing PDA solid medium inoculated only with *F. graminearum* in the center served as the negative controls. For the experimental groups, purified isolates were added to the medium edge symmetrically from the center. All Petri dishes were incubated in the dark at 25 °C until the PDA medium for the negative controls was completely covered by *F. graminearum*. The radial growth of *F. graminearum* in the control (R1) and experimental groups (R2) was then measured with a ruler. The inhibition rate of radial growth of *F. graminearum* by the isolated bacteria was calculated as follows: $100 \times [(R1 - R2)/R1]$.

Examining the influence of beneficial *bacteria* on plant disease

The purified isolates that showed antagonistic activity against *F. graminearum* were cultured in LB broth at 28 °C for 12 h, centrifuged at 25 °C for 2 min at 7000 g, and resuspended in sterile water to an OD_{600} value of 1.0. Maize seeds from a CSR-resistant cultivar GZL455 were surface sterilized by soaking for 5 min in 8.25% NaClO, followed by one rinse with sterilized distilled water, a single rinse of 70% ethanol, and three rinses with sterile distilled water. Surface-sterilized maize seeds were incubated in Petri dishes with distilled water at 25 °C for 3 days for germination. For the negative controls, 2 mL of distilled water was added to the soil around the maize seeds. Maize seeds treated with 2 mL of *F. graminearum* spore suspension at a concentration of 10^8 spores/mL served as the positive controls. To examine the effects

of beneficial bacteria on CSR development, *F. graminearum* (2 mL, 2×10^5 spores/mL) and pure beneficial bacteria (2 mL, $OD_{600}=1.0$) were added simultaneously to the root tips. All maize seeds were planted in plastic cones containing sterile substrate amended with roseite in the greenhouse. Cones with the same treatment were arranged randomly in plastic racks and incubated in a growth chamber (14 h light/10 h dark) at 26 °C. The disease severity of the maize plants was assessed based on the number of diseased plants after 2 weeks.

RNA-seq of maize roots after inoculation with a synthetic community of *bacteria*

Three strains from the three groups (SC-I: 455–535, 339–154, 339–288; SC-II: 455–565, 339–97, 339–233; and SC-III: 339–229, 455–332, 455–62) of *Bacillus* were selected to construct three SCs. Briefly, the selected bacterial strains were individually grown on LB solid medium at 28 °C. Then, the single colonies were individually propagated in TSB medium using the shake flask fermentation method with an overall culture period of 24 h at 25 °C. Each of the bacterial fermentation broth was centrifuged at 4000 g for 5 min and re-suspended in sterile water with OD_{600} adjusted to 0.02 (~ 10^7 cells/mL). The SC inoculum was obtained by combining 3 bacterial strains of the same group as above in equal suspension volumes. The optical density (OD_{600}) of the SC inoculum was adjusted to 0.02 with sterile water. A 20 mL aliquot of SC suspension was poured onto the roots of 2-week-old maize seedlings from a CSR-resistant cultivar GZL455 growing in sterile substrate. The control groups received equal amounts of sterile water. Twenty-four hours after inoculation, the plants were uprooted from the substrate soil, and the roots were washed in phosphate-buffered saline (PBS) buffer. Clean roots separated from the rest of the plant with five biological replicates were flash-frozen in liquid nitrogen and stored at − 80 °C. TRIzol reagent (1.5 mL) was used to extract total RNA from the root tissues, and the integrity and purity of the RNA were assessed using an Agilent 2100 Bioanalyzer (Agilent Technologies, CA, USA) and a NanoPhotometer Spectrophotometer (IMPLEN, CA, USA), respectively. A 1 μg aliquot of RNA per sample was used as input material for the RNA sample preparations. Sequencing libraries were generated using an NEBNext Ultra RNA Library Prep Kit from Illumina (NEB, USA) following the manufacturer's recommendations, and index codes were added to attribute sequences to particular samples. Following purification and quality assessment, the library was sequenced on the Illumina NovaSeq platform, and 150-bp paired-end reads were generated.

Clean reads were obtained by removing reads containing adapters, reads containing poly-N, and low-quality reads from the raw data. Clean paired-end reads were aligned to the B73 maize genome v5.0, which was downloaded from maize GDB, using Hisat2v 2.0.5 [76]. StringTie v 2.2.1 [77] was used to count the number of reads mapped to each gene, and the fragments per kilobase of transcript per million mapped reads (FPKM) value of each gene were calculated based on the length of the gene. Differential expression analysis was performed using the R package DESeq2 v1.16.1. Gene Ontology (GO) and KEGG enrichment analysis of differentially expressed genes (DEGs) were performed using the R package clusterProfiler v4.1.2, in which gene length bias was corrected. Functional terms with corrected *P*-values < 0.05 were considered to be significantly enriched. The expression of genes in core pathways was further verified by reverse-transcription quantitative PCR (RT-qPCR). Briefly, the SC-associated experiment described above including RNA preparation was performed again. A HiScript III 1st Strand cDNA Synthesis Kit (Vazyme, Nanjing, China) and RealStar Green Fast Mixture with ROXII (GenStar, Beijing, China) were employed for cDNA synthesis and qPCR, respectively. The $2^{-\Delta\Delta Ct}$ method was used to determine the relative expression levels of the target genes.

Effects of berberine on pathogen growth and the occurrence of CSR

To evaluate the effects of specific root exudates on pathogen growth, four PDA plates containing 5, 25, 50, or 100 μg/mL berberine (Solarbio) were prepared, and 5% (v/v) DMSO was added to the PDA as the mock treatment. Agar disks containing fresh mycelium were inoculated into the centers of the PDA plates with four replicates per treatment, and the plates were incubated at 25 °C for 48 h.

For greenhouse experiments, maize seeds (the CSR-susceptible cultivar, GZL200) were surface sterilized by soaking for 5 min in 8.25% NaClO, followed by one rinse with sterilized distilled water, a single rinse of 70% ethanol, and three rinses with sterile distilled water. The seeds were soaked in 25 μg/mL berberine solution for 5 min and planted in the sterile substrate. Roots were inoculated by irrigation with *F. graminearum* (2 mL, 2×10^5 spores/mL) at 3 days after planting. CSR incidence was scored with the naked eye and recorded every 5 days.

Statistical analyses

The statistically significant differences in bacterial community composition, plant biomass, and SDI between CSR-resistant and CSR-susceptible groups were evaluated by a two-tailed unpaired Wilcoxon rank sum test at a threshold *P*-value < 0.05. Differential abundance of the metabolites in the rhizosphere and root endosphere

between CSR-resistant and CSR-susceptible groups was calculated using the generalized linear model (GLM) approach in the R package edge R v3.34.1. The major drivers of microbial and fungal alpha-diversity were determined by linear mixed model analysis using the R package lme4 v4.1.3. The β-diversity of bacterial and fungal communities and the functional categories were assessed by computing the Bray–Curtis distance matrices and then ordinated using PCoA. PERMANOVA statistical tests were performed to determine the relative contributions of different factors to community dissimilarity using Adonis in the R package Vegan v4.1.3 with 1999 permutations. The biomarker bacteria were identified using LEfSe (logarithmic LDA score > 2.5, *P*-value < 0.05).

Supplementary Information

The online version contains supplementary material available at https://doi.org/10.1186/s40168-024-01887-w.

Additional file 1: Extended Data Fig. 1. Bacterial and fungal βNTI information, niche widths, diffusional limitation and Shannon diversities in bacterial and fungal communities. (a) Pot experiments were performed to validate the importance of soil microbiome for CSR-resistance by planting the four CSR-resistant cultivars into natural and sterile soil. (b) βNTI calculations of phylogenetic turnover among bacterial (left) and fungal (right) samples in the five maize compartments: BS, bulk soil; RS, rhizosphere soil; RE, root endosphere; SE, stem endosphere; GE, grain endosphere. For pairwise comparisons in the Wilcoxon rank sum test, a and b correspond to $P < 0.05$; ns corresponds to $P > 0.05$. (c) Niche widths of bacterial communities among the five compartments. (d) Predicted frequencies of occurrence for CSR-resistant and CSR-susceptible communities in the five compartments. The solid blue lines are the best fit to the neutral community model (NCM), and the dashed blue lines indicate 95% confidence intervals around the NCM prediction. OTUs that occur more or less frequently than predicted by the NCM are shown in green and red, respectively. R^2 represents the fit to this model. Nm represents the quantitative estimate of diffusional limitation. (e) Shannon diversity index (SDI) values in CSR-resistant and CSR-susceptible samples in bacterial and fungal communities among the five compartments.

Additional file 2: Extended Data Fig. 2. Core fungal taxa in CSR-resistant and CSR-susceptible groups. (a) The interactive degree of *Fusarium* from the bacteria-fungi co-occurrence networks. (b) Cladograms indicating the phylogenetic distribution of the bacterial lineages in the CSR-resistant (R, green) and CSR-susceptible (S, magenta) maize cultivars. The taxa with an LDA score > 2.5 were selected as biomarkers to distinguish the CSR-resistant and CSR-susceptible groups. (c) Number of shared and specific genera showing differences in abundance between fungal groups associated with CSR-resistant and CSR-susceptible cultivars (Wilcox test, $P < 0.05$). (d) Relative abundance of *Alternaria*, *Nigrospora* and *Trichoderma* among the five compartments. Data are shown as mean ± SEM ($n = 20$). Pairwise significant differences were analyzed using a Wilcoxon rank sum test (* $P < 0.05$, ** $P < 0.01$, *** $P < 0.001$).

Additional file 3: Extended Data Fig. 3. *Bacillus* species positively affect plant CSR-resistance to *F. graminearum*. (a) Phenotypic characteristics of healthy and infected maize seedlings at 2 weeks following inoculation with *F. graminearum*. (b–d) Mean emergence rates (b), dry root weights (c) and fresh root weights are shown as mean ± SD. Different letters indicate significant differences (ordinary one-way ANOVA test, $P < 0.05$).

Additional file 4**:** Extended Data Fig. 4. Verification of the transcriptomic results by RT-qPCR and disease suppression by berberine. (a–b) Tree maps of the GSEA functional terms of maize roots treated with SC-I (a) or SC-II (b); the sizes of boxes correspond to the number of core genes related to each functional term. The NES values are shown under the functional pathway name. (c) Relative expression levels of selected genes across treatments in maize roots, as determined by RT-qPCR. Results are shown as mean ± SD. Different letters indicate significant differences (ordinary one-way ANOVA test, $P < 0.05$). (d) Normalized concentrations of key compounds related to berberine biosynthesis, as determined by LC–MS/MS. Pairwise significant differences were analyzed using a Wilcoxon rank sum test (* $P < 0.05$, ** $P < 0.01$, *** $P < 0.001$). (e) Diameters of mycelia grown on *F. graminearum* on PDA assay plates supplemented with no, 5, 25, 50 or 100 μg/mL berberine. Results are shown as mean ± SD. Different letters indicate significant differences (ordinary one-way ANOVA test, $P < 0.05$).

Additional file 5: Supplementary Table 1. Detailed pedigree information of an association mapping panel (AMP) consisting of 527 diverse cultivars. The 527 cultivars contains different populations, including 33 lines for stiff-stock (SS), 143 for non-stiff-stock (NSS), 232 for tropical and semi-tropical (TST) and the left 119 lines for mixed. Supplementary Table 2. Detailed pedigree information and CSR disease indexes over two consecutive years for 40 cultivars obtained from an association mapping panel consisting of 527 diverse cultivars. Supplementary Table 3. Results of linear mixed model analysis to examine which major factors shape the maize microbiota. Supplementary Table 4. Statistics of the p-values of pairwise multilevel comparison using Adonis across the eight cultivars in bacterial and fungal communities. Supplementary Table 5. Wilcox test results of βNTI between CSR-resistant and CSR-susceptible groups among the five compartments. Supplementary Table 6. Tukey's multiple comparisons test of the SDIs comparing two compartments. Supplementary Table 7. Pairwise multilevel comparison between two compartments using Adonis. Supplementary Table 8. Pairwise multilevel comparison between CSR-resistant and CSR-susceptible cultivars in the same compartments using Adonis. Supplementary Table 9. Statistical information about the syncretic bacterial–fungal co-occurrence networks. Supplementary Table 10. Number of shared OTUs and unique edges plus their dissimilarity between CSR-resistant and CSR-susceptible maize cultivars in the five compartments. Supplementary Table 11. The core bacterial and fungal taxa that appeared in more than 80% samples. Supplementary Table 12. Taxonomies of the 276 isolates from two CSR-resistant maize cultivars based on 16S rRNA gene sequencing. Supplementary Table 13. GSEA enrichment results from maize roots treated with SC-I, SC-II or SC-III. Supplementary Table 14. Metabolites from the root endogenous samples of CSR-resistant and CSR-susceptible maize cultivars from Jilin Province in 2021, as determined by LC–MS/MS. Supplementary Table 15. Metabolites from the rhizosphere samples of CSR-resistant and CSR-susceptible maize cultivars from Jilin Province in 2021, as determined by LC–MS/MS.

Acknowledgements
We thank Prof. Changlong SHU (Institute of Plant Protection, Chinese Academy of Agricultural Sciences) for his technical support on the identification of Bacillus isolates. We also thank Yan's lab from Huazhong Agricultural University and Yang's lab from China Agricultural University for providing seeds of the inbred lines.

Authors' contribution
Wende Liu, Wenxian Sun conceived and designed the study. Xinyao Xia, Qiuhe Wei, Hanxiang Wu, Xinyu Chen, Chunxia Xiao, Chaotian Liu and Haiyue Yu performed the experiments and analyzed the data. Wende Liu, Hanxiang Wu, Xinyao Xia and Qiuhe Wei wrote the manuscript with contributions from all the other authors.

Funding
This work was financially supported by the National Key R&D Program of China (2022YFD1402000), and the Agricultural Science and Technology Innovation Program of the Chinese Academy of Agricultural Sciences.

Availability of data and materials
Sequencing data from this study can be found in NCBI under the following BioProject numbers: PRJNA990978, including the 16S rRNA gene sequencing data (SAMN36289239-SAMN36289436), ITS rRNA sequencing data (SAMN36377919-SAMN36378116), transcriptomic data (SAMN36399084-SAMN36399095) and metagenomic data (SAMN36381305-SAMN36381346). Metadata, the unrarefied OTU table, corresponding taxonomic classifications

and original R scripts for all samples used in this study have been deposited in Zenodo (https://zenodo.org/records/11497461).

Declarations

Ethics approval and consent to participate
Not applicable.

Consent for publication
Not applicable.

Competing interests
The authors declare no competing interests.

Received: 20 November 2023 Accepted: 27 July 2024
Published online: 23 August 2024

References

1. Lu ZX, Tu GP, Zhang T, et al. Screening of antagonistic Trichoderma strains and their application for controlling stalk rot in maize. J Integr Agric. 2020;19(1):145–52.
2. Martinez-Cisneros BA, Juarez-Lopez G, Valencia-Torres N, Duran-Peralta E, Mezzalama M. First report of bacterial stalk rot of maize caused by Dickeya zeae in Mexico. Plant Dis. 2014;98(9):1267–367.
3. Li-Ping Y, Gen-Hua Y, Zhi-Lin LI, Hua X, Rong-Cai MA. Isolation and characterization of a new Pseudomonas aeruginosa strain from bacterial stalk rotted maize. J Agric Sci Technol. 2014;16(1):65–70.
4. Haryuni H, Harahap AFP, Supartini, Priyatmojo A, Gozan M. The effects of Biopesticide and fusarium oxysporum f. sp. vanillae on the nutrient content of binucleate rhizoctonia-induced vanilla plant. Int J Agron. 2020;2020:1–6.
5. Jackson-Ziems TA, Giesler LJ, Harveson RM, Wegulo SN, Korus K, Adesemoye AO. Fungicide application timing and disease control. 2016.
6. Huet G. Breeding for resistances to Ralstonia solanacearum. Front Plant Sci. 2014;5:715.
7. Muthoni J, Shimelis H, Melis R. Conventional breeding of potatoes for resistance to bacterial wilt ('Ralstonia solanacearum'): any light in the horizon? Aust J Crop Sci. 2020;14(3):485–94.
8. del Carmen Orozco-Mosqueda M, Fadiji AE, Babalola OO, Glick BR, Santoyo G. Rhizobiome engineering: unveiling complex rhizosphere interactions to enhance plant growth and health. Microbiol Res. 2022;263:127137.
9. Hassani M, Durán P, Hacquard S. Microbial interactions within the plant holobiont. Microbiome. 2018;6(1):1–17.
10. Bai B, Liu W, Qiu X, Zhang J, Zhang J, Bai Y. The root microbiome: community assembly and its contributions to plant fitness. J Integr Plant Biol. 2022;64(2):230–43.
11. Wang Z, Song Y. Toward understanding the genetic bases underlying plant-mediated "cry for help" to the microbiota. IMeta. 2022;1(1):e8.
12. Kwak M-J, Kong HG, Choi K, et al. Rhizosphere microbiome structure alters to enable wilt resistance in tomato. Nat Biotechnol. 2018;36(11):1100–9.
13. Eid AM, Salim SS, Hassan SED, Ismail MA, Fouda A. Role of endophytes in plant health and abiotic stress management. In: Microbiome in plant health and disease: challenges and opportunities. 2019. p. 119–44.
14. Song Y, Wilson AJ, Zhang X-C, et al. FERONIA restricts Pseudomonas in the rhizosphere microbiome via regulation of reactive oxygen species. Nature Plants. 2021;7(5):644–54.
15 Feng H, Fu R, Luo J, et al. Listening to plant's Esperanto via root exudates: reprogramming the functional expression of plant growth-promoting rhizobacteria. New Phytol. 2023;239:2307–19.
16. Karuppiah V, He A, Lu Z, Wang X, Li Y, Chen J. Trichoderma asperellum GDFS1009-mediated maize resistance against Fusarium graminearum stalk rot and mycotoxin degradation. Biol Control. 2022;174:105026.
17 Dubey SC, Suresh M, Singh B. Evaluation of Trichoderma species against Fusarium oxysporum f. sp. ciceris for integrated management of chickpea wilt. Biol Control. 2007;40(1):118–27.
18. Gao M, Xiong C, Gao C, et al. Disease-induced changes in plant microbiome assembly and functional adaptation. Microbiome. 2021;9:1–18.
19. Damodaran T, Rajan S, Muthukumar M, et al. Biological management of banana Fusarium wilt caused by Fusarium oxysporum f. sp. cubense tropical race 4 using antagonistic fungal isolate CSR-T-3 (Trichoderma reesei). Front Microbiol. 2020;11:595845.
20. Zha Y, Chong H, Yang P, Ning K. Microbial dark matter: from discovery to applications. Genomics Proteomics Bioinformatics. 2022;20(5):867–81.
21. Yuan J, Zhao J, Wen T, et al. Root exudates drive the soil-borne legacy of aboveground pathogen infection. Microbiome. 2018;6(1):1–12.
22. Wassermann B, Cernava T, Müller H, Berg C, Berg G. Seeds of native alpine plants host unique microbial communities embedded in cross-kingdom networks. Microbiome. 2019;7(1):1–12.
23. Yang K, Fu R, Feng H, et al. RIN enhances plant disease resistance via root exudate-mediated assembly of disease-suppressive rhizosphere microbiota. Mol Plant. 2023;16:1379–95.
24. Yang X, Gao S, Xu S, et al. Characterization of a global germplasm collection and its potential utilization for analysis of complex quantitative traits in maize. Mol Breeding. 2011;28:511–26.
25. Wen T, Xie P, Penton CR, et al. Specific metabolites drive the deterministic assembly of diseased rhizosphere microbiome through weakening microbial degradation of autotoxin. Microbiome. 2022;10(1):1–15.
26. Shen Z, Thomashow LS, Ou Y, et al. Shared core microbiome and functionality of key taxa suppressive to banana Fusarium wilt. Research. 2023;1:15.
27. French E, Kaplan I, Iyer-Pascuzzi A, Nakatsu CH, Enders L. Emerging strategies for precision microbiome management in diverse agroecosystems. Nature plants. 2021;7(3):256–67.
28. Wagner MR, Lundberg DS, Del Rio TG, Tringe SG, Dangl JL, Mitchell-Olds T. Host genotype and age shape the leaf and root microbiomes of a wild perennial plant. Nat Commun. 2016;7(1):12151.
29. Wang Y, Wang X, Sun S, et al. GWAS, MWAS and mGWAS provide insights into precision agriculture based on genotype-dependent microbial effects in foxtail millet. Nat Commun. 2022;13(1):5913.
30 Zhang J, Liu YX, Zhang N, et al. NRT1. 1B is associated with root microbiota composition and nitrogen use in field-grown rice. Nat Biotechnol. 2019;37(6):676–84.
31. Matarese F, Sarrocco S, Gruber S, Seidl-Seiboth V, Vannacci G. Biocontrol of Fusarium head blight: interactions between Trichoderma and mycotoxigenic Fusarium. Microbiology. 2012;158(1):98–106.
32 Nakkeeran S, Rajamanickam S, Saravanan R, Vanthana M, Soorianathasundaram K. Bacterial endophytome-mediated resistance in banana for the management of Fusarium wilt. 3 Biotech. 2021;11(6):267.
33. Larkin RP, Fravel DR. Efficacy of various fungal and bacterial biocontrol organisms for control of Fusarium wilt of tomato. Plant Dis. 1998;82(9):1022–8.
34 d'Enfert C, Kaune A-K, Alaban L-R, et al. The impact of the Fungus-Host-Microbiota interplay upon Candida albicans infections: current knowledge and new perspectives. FEMS Microbiol Rev. 2021;45(3):fuaa060.
35. Tewksbury JJ, Reagan KM, Machnicki NJ, et al. Evolutionary ecology of pungency in wild chilies. Proc Natl Acad Sci. 2008;105(33):11808–11.
36. Sokol NW, Slessarev E, Marschmann GL, et al. Life and death in the soil microbiome: how ecological processes influence biogeochemistry. Nat Rev Microbiol. 2022;20(7):415–30.
37. Freilich MA, Wieters E, Broitman BR, Marquet PA, Navarrete SA. Species co-occurrence networks: can they reveal trophic and non-trophic interactions in ecological communities? Ecology. 2018;99(3):690–9.
38. Zhu W, Zhu M, Liu X, Xia J, Yin H, Li X. Different responses of bacteria and microeukaryote to assembly processes and co-occurrence pattern in the coastal upwelling. Microb Ecol. 2023;86(1):174–86.
39. Yuan MM, Kakouridis A, Starr E, et al. Fungal-bacterial cooccurrence patterns differ between arbuscular mycorrhizal fungi and nonmycorrhizal fungi across soil niches. MBio. 2021; 12(2):https://doi.org/10.1128/mbio.03509-20
40. Foroud NA, Chatterton S, Reid LM, Turkington TK, Tittlemier SA, Gräfenhan T. Fusarium diseases of Canadian grain crops: impact and disease management strategies. In: Future challenges in crop protection against fungal pathogens. 2014. p. 267–316.
41. Khan N, Maymon M, Hirsch AM. Combating Fusarium infection using Bacillus-based antimicrobials. Microorganisms. 2017;5(4):75.

42. Chowdhury SP, Hartmann A, Gao X, Borriss R. Biocontrol mechanism by root-associated Bacillus amyloliquefaciens FZB42–a review. Front Microbiol. 2015;6:780.
43 Ramírez V, Martínez J, Bustillos-Cristales MDR, Catañeda-Antonio D, Munive JA, Baez A. Bacillus cereus MH778713 elicits tomato plant protection against Fusarium oxysporum. J Appl Microbiol. 2022;132(1):470–82.
44. Abada EA, Elbaz RM, Sonbol H, Korany SM. Optimization of cellulase production from Bacillus albus (MN755587) and its involvement in bioethanol production. Pol J Environ Stud. 2021;30(3):2459–66.
45. Bacon CW, Hinton DM. Endophytic and biological control potential of Bacillus mojavensis and related species. Biol Control. 2002;23(3):274–84.
46 Akhtar MS, Siddiqui ZA. Glomus intraradices, Pseudomonas alcaligenes, and Bacillus pumilus: effective agents for the control of root-rot disease complex of chickpea (Cicer arietinum L.). J Gen Plant Pathol. 2008;74:53–60.
47 Schwartz AR, Ortiz I, Maymon M, et al. Bacillus simplex—a little known PGPB with anti-fungal activity—alters pea legume root architecture and nodule morphology when coinoculated with Rhizobium leguminosarum bv. viciae. Agronomy. 2013;3(4):595–620.
48. Nazli F, Wang X, Ahmad M, et al. Efficacy of indole acetic acid and exopolysaccharides-producing Bacillus safensis strain FN13 for inducing Cd-stress tolerance and plant growth promotion in Brassica juncea (L.). Appl Sci. 2021;11(9):4160.
49. Jiao H, Xu W, Hu Y, Tian R, Wang Z. Citric acid in rice root exudates enhanced the colonization and plant growth-promoting ability of Bacillus altitudinis LZP02. Microbiol Spectrum. 2022;10(6):e01002-e1022.
50. Nobori T, Cao Y, Entila F, et al. Dissecting the cotranscriptome landscape of plants and their microbiota. EMBO Rep. 2022;23(12):e55380.
51. Trivedi P, Batista BD, Bazany KE, Singh BK. Plant–microbiome interactions under a changing world: responses, consequences and perspectives. New Phytol. 2022;234(6):1951–9.
52. Liu H, Brettell LE, Qiu Z, Singh BK. Microbiome-mediated stress resistance in plants. Trends Plant Sci. 2020;25(8):733–43.
53. Yu P, He X, Baer M, et al. Plant flavones enrich rhizosphere Oxalobacteraceae to improve maize performance under nitrogen deprivation. Nature plants. 2021;7(4):481–99.
54. Yue R, Lu C, Han X, et al. Comparative proteomic analysis of maize (Zea mays L.) seedlings under rice black-streaked dwarf virus infection. BMC Plant Biol. 2018;18:1–11.
55. Cao A, Gesteiro N, Santiago R, Malvar RA, Butron A. Maize kernel metabolome involved in resistance to fusarium ear rot and fumonisin contamination. Front Plant Sci. 2023;14:1160092.
56. Zhang C, Ou X, Wang J, et al. Antifungal peptide P852 controls Fusarium wilt in faba bean (Vicia faba L.) by promoting antioxidant defense and isoquinoline alkaloid, betaine, and arginine biosyntheses. Antioxidants. 2022;11(9):1767.
57. Yang N, Liu J, Gao Q, et al. Genome assembly of a tropical maize inbred line provides insights into structural variation and crop improvement. Nat Genet. 2019;51(6):1052–9.
58. Caporaso JG, Kuczynski J, Stombaugh J, et al. QIIME allows analysis of high-throughput community sequencing data. Nat Methods. 2010;7(5):335–6.
59. Edgar RC. Search and clustering orders of magnitude faster than BLAST. Bioinformatics. 2010;26(19):2460–1.
60. Brown J, Pirrung M, McCue LA. FQC Dashboard: integrates FastQC results into a web-based, interactive, and extensible FASTQ quality control tool. Bioinformatics. 2017;33(19):3137–9.
61. Bolger AM, Lohse M, Usadel B. Trimmomatic: a flexible trimmer for Illumina sequence data. Bioinformatics. 2014;30(15):2114–20.
62. Quast C, Pruesse E, Yilmaz P, et al. The SILVA ribosomal RNA gene database project: improved data processing and web-based tools. Nucleic Acids Res. 2012;41(D1):D590–6.
63. Nilsson RH, Larsson KH, Taylor AFS, et al. The UNITE database for molecular identification of fungi: handling dark taxa and parallel taxonomic classifications. Nucleic Acids Res. 2019;47(D1):D259–64.
64. Ihaka R, Gentleman R. R: a language for data analysis and graphics. J Comput Graph Stat. 1996;5(3):299–314.
65. Bastian M, Heymann S, Jacomy M, editors. Gephi: an open source software for exploring and manipulating networks. Proceedings of the international AAAI conference on web and social media; 2009.
66. Mendes LW, Mendes R, Raaijmakers JM, Tsai SM. Breeding for soil-borne pathogen resistance impacts active rhizosphere microbiome of common bean. ISME J. 2018;12(12):3038–42.
67. Poisot T, Canard E, Mouillot D, Mouquet N, Gravel D. The dissimilarity of species interaction networks. Ecol Lett. 2012;15(12):1353–61.
68. Mo Y, Peng F, Gao X, et al. Low shifts in salinity determined assembly processes and network stability of microeukaryotic plankton communities in a subtropical urban reservoir. Microbiome. 2021;9(1):1–17.
69. Li D, Liu C-M, Luo R, Sadakane K, Lam T-W. MEGAHIT: an ultra-fast single-node solution for large and complex metagenomics assembly via succinct de Bruijn graph. Bioinformatics. 2015;31(10):1674–6.
70. Hyatt D, Chen GL, Locascio PF, Land ML, Larimer FW, Hauser LJ. Prodigal: prokaryotic gene recognition and translation initiation site identification. BMC Bioinformatics. 2010;11(1):119–219.
71. Li W, Godzik A. Cd-hit: a fast program for clustering and comparing large sets of protein or nucleotide sequences. Bioinformatics. 2006;22(13):1658–9.
72. Kessner D, Chambers M, Burke R, Agus D, Mallick P. ProteoWizard: open source software for rapid proteomics tools development. Bioinformatics. 2008;24(21):2534–6.
73. Bankevich A, Nurk S, Antipov D, et al. SPAdes: a new genome assembly algorithm and its applications to single-cell sequencing. J Comput Biol. 2012;19(5):455–77.
74. Seemann T. Prokka: rapid prokaryotic genome annotation. Bioinformatics. 2014;30(14):2068–9.
75. Wang K, Shu C, Bravo A, et al. Development of an online genome sequence comparison resource for Bacillus cereus sensu lato strains using the efficient composition vector method. Toxins. 2023;15(6):393.
76. Kim D, Paggi JM, Park C, Bennett C, Salzberg SL. Graph-based genome alignment and genotyping with HISAT2 and HISAT-genotype. Nat Biotechnol. 2019;37(8):907–15.
77. Pertea M, Pertea GM, Antonescu CM, Chang T-C, Mendell JT, Salzberg SL. StringTie enables improved reconstruction of a transcriptome from RNA-seq reads. Nat Biotechnol. 2015;33(3):290–5.

Publisher's Note